Population differentiation and structural variation in the *Manduca sexta* genome across the United States

Andrew J. Mongue[*†], Akito Y. Kawahara[‡]

[*] University of Edinburgh, Institute of Evolutionary Biology, Edinburgh, UK, EH93FL

[†] University of Kansas, Department of Ecology and Evolutionary Biology, Lawrence, KS, USA, 66045

[‡]McGuire Center for Lepidoptera and Biodiversity, Florida Museum of Natural History, University of Florida, Gainesville, FL 32611

Running title: Segregating inversions in *Manduca sexta*

Keywords: tobacco hornworm, Carolina sphinx moth, inversion, sex chromosomes, pseudogene, resequencing, population structure, agricultural entomology

correspondence contact: Andrew J. Mongue

Ashworth 2.02, Charlotte Auerbach Road, Edinburgh, UK, EH93FL

+1-906-241-2776

ajmongue@gmail.com

Abstract

Many species that are extensively studied in the laboratory are less well characterized in their natural habitat, and laboratory strains represent only a small fraction of the variation in a species' genome. Here we investigate genomic variation in three natural North American populations of an agricultural pest and a model insect for many scientific disciplines, the tobacco hornworm (*Manduca sexta*). We show that hornworms from Arizona, Kansas, and North Carolina are genetically distinct, with Arizona being particularly differentiated from the other two populations using Illumina whole-genome resequencing. Peaks of differentiation exist across the genome, but here we focus in on the most striking regions. In particular, we identify two likely segregating inversions found in the Arizona population. One inversion on the Z chromosome may enhance adaptive evolution of the sex chromosome. The larger, autosomal inversion contains a pseudogene may be involved in the exploitation of a novel hostplant in Arizona, but functional genetic assays will be required to support this hypothesis. Nevertheless, our results reveal undiscovered natural variation and provide useful genomic data for both pest management and evolutionary genetics of this insect species.

Introduction

One of the main objectives of evolutionary genetics is to unite the proximate molecular function of genes with the long-term evolutionary forces that govern their change (Nei 1987). The two halves of this pursuit necessitate different approaches, with well-controlled laboratory studies best suited to elucidating the biochemistry of gene function and surveys of natural variation required to understand the ecological and demographic context in which these genes exist. The most fruitful species to study in the lab tend to be those with small body sizes and short generation times. In the field, common species with large population sizes are easiest to sample. Consequently, many of the most popular models for evolutionary genetics come from insects, which fulfill all of the above criteria.

For a brief example, consider the well-studied flies in the genus *Drosophila*. Early pioneers of evolutionary genetics noted that *Drosophila* collected from different locations often had differing arrangements of genes along their chromosomes, in other words, inversion polymorphisms within and between populations (Sturtevant 1917; Dobzhansky and Sturtevant 1938). But without the context provided by population genomic methods, these authors could only catalog the various structural rearrangements they observed; the evolutionary significance of these traits was unknown. With the benefit of modern sequencing technologies, researchers have since shown that segregating inversions like these often exist in environmental clines and contribute to maintaining fitness across a variety of environmental conditions (Anderson *et al.* 2005; Kapun *et al.* 2016; Wellenreuther *et al.* 2017). The initial discovery could only come from controlled laboratory crosses, but the significance could only be established by studying individuals taken from natural populations.

In spite of successes like these, species for which both robust natural and controlled studies exist remain rare. Certainly, the establishment of a new laboratory model species is a massive undertaking and model status can only be achieved through widespread adoption in the research community, which takes years if not decades. Conversely, population genetic sampling is only becoming more tractable with advances in sequencing technology. From this perspective, it is more logical to identify well-studied species that lack population genetic data and bring that natural context to them.

The tobacco hornworm moth (*Manduca sexta*) is a well-established laboratory model (Reinecke, Buckner, & Grugel, 1980), and likely the second most studied moth after the domestic silkmoth, *Bombyx mori* (The International Silkworm Genome Consortium, 2008). The tobacco hornworm is used to study developmental biology of numerous organs (Höglund and Struwe 1970; Banister and White 1987; Nardi 1993), immunology (Kanost *et al.* 2004), reproductive biology (Whittington *et al.* 2015; Mongue and Walters 2017), along with a range of other topics. This attention has resulted in a wealth of genetic information for this species, with many physiological functions characterized by the genetic pathways on which they depend and supported by robust sequencing of RNA (aggregated in Cao and Jiang 2017). In other words, there has been great progress in understanding the molecular genetics of this species.

Yet for all of this research in vitro, the genetics of *M. sexta* in its natural habit remains largely unexplored. Its phylogenetic relationship to other sphinx moths was only recently genetically evaluated (Kawahara *et al.* 2013) and only two years ago were the first whole genome sequences from wild individuals generated (Mongue *et al.* 2019). Very basic questions of natural populations have yet to be addressed. For instance, *M. sexta*, like other moths in the family Sphingidae are particularly strong and mobile fliers (Stevenson *et al.* 1995) and at one time it was claimed that this species is migratory (Ferguson 1991). However, both this initial claim and its later refutation are based solely on limited observations of seasonal occurrence (McNeil 1995) and the ability of pupae to survive subfreezing temperatures (Shapiro 2006). Surprisingly, there have been no genetic studies of population structuring of *M. sexta* to date.

This lack of research into the population genetics of this moth is puzzling on two fronts. First, in terms of basic research, much of the ecological knowledge about this moth, such as acclimation and adaptation to different environments and host plants (Mechaber and Hildebrand 2000; Contreras *et al.* 2013) could benefit from understanding natural genetic variation across its range. Second, as the name tobacco hornworm suggests, *M. sexta* is a pest of economically important crops, including tobacco (*Nicotiana* spp.), tomatoes, peppers, and generally other plants in the nightshade family, Solanaceae (Wagner 2005). Thus, understanding how *M. sexta* populations are structured will inform pest management strategies. In service of both of these goals, we present whole-genome resequencing of this model insect to investigate population structure across an east-west transect of the continental United States. With these resequencing samples, we establish patterns of regional genetic variation and differentiated parts of the genome for further studies of *M. sexta.*

Methods

Sample collection and sequencing

For an initial characterization of genetic variation in this broadly distributed species, samples were chosen, based on availability, to maximize the geographic range represented while still sampling local populations with enough individuals to detect large changes in allele frequency. Specifically, samples from three states in the US were examined in this project: North Carolina (n = 12), Kansas (n = 4), and Arizona (n = 8); see Figure 1. Collecting methods varied somewhat between these locales. Samples from North Carolina were already obtained and sequenced as part of Mongue *et al.* (2019). In brief, adults were collected over the course of a week from a mercury vapor light trap in a single locale in July of 2017. Kansas samples were obtained from a mixture of adult moths caught at light traps and larvae taken from tomato fields in different towns in eastern Kansas throughout the summer of 2018. For larval

140 sampling, only one individual was sequenced per field to minimize the risk of sequencing siblings.
141 Arizona samples were obtained from the University of Florida's collections, where adult moths had been
142 preserved in ethanol. At time of collection, they were collected from a mercury vapor trap at one
143 location over several nights in July of 2012. A summary of sequenced individuals and their methods of
144 collection can be found in Table 1.

145 For each sample, tissue was extracted from adult thoracic flight muscle to avoid eggs and sperm in the
146 abdomen, and larval head capsules to avoid hostplant tissue in the gut. DNA was extracted using an
147 Omniprep kit for genomic DNA (G-Biosciences, St. Louis, MO, USA), following the manufacturer's
148 protocol. DNA was isolated via phase-separation with chloroform and precipitated with ethanol. DNA
149 pellets were resuspended in buffer and sent for Illumina sequencing with Novogene Sequencing
150 (Sacramento, CA, USA). Quality control and library preparation followed the company's standard and
151 sequencing generated 150 basepair, paired-end reads sequenced to an average depth of 14-20x
152 coverage across the genome (also summarized in Table 1). As part of the sequencing service, the
153 company trimmed raw reads for both quality and adapter sequence content.

154 Starting points for genomic analyses

155 Recent work on the *Manduca sexta* genome assembly has created both the opportunity and need for
156 some comparative work on the multiple available assemblies. *Manduca sexta* has had an Illumina-only
157 (i.e. fragmented) genome assembly for several years (Kanost *et al.* 2016); much more recently a
158 chromosome-level assembly has been published (Gershman *et al.* 2021). Naturally, the chromosome-
159 level assembly's more contiguous scaffolds facilitate identification of large-scale variation; however, the
160 previous assembly features high quality gene models informed by dozens of RNA-sequencing
161 experiments and manually updated over the last five years (Kanost *et al.* 2016). To take advantage of the
162 strengths of both assemblies, the same analysis pipeline was carried out on both assemblies to leverage
163 the wealth of available data. Generally speaking, the newer assembly was employed for genome-wide
164 investigation of differentiation and the older assembly was used to validate patterns observed in the
165 former and investigate specific gene(set)s of interest. For both assemblies, the same processed short-
166 read data were aligned to the reference using the very-sensitive-local alignment setting in Bowtie2
167 version 2.2.9 (Langmead & Salzberg, 2012). Alignments were coordinate-sorted and optical duplicates
168 were removed with Picardtools v. 2.8 (Wysoker *et al.* 2013). Finally, alignments around insertions and
169 deletions were adjusted with GATK v. 3.7 (McKenna et al., 2010). This end result generated a set of
170 curated alignment files (bams) that were the starting point for all downstream analyses.

171 For some of these analyses, it was necessary to analyze the genotypes of single nucleotide variants. To
172 generate sets of high-confidence variants, the curated alignments were taken through GATK v 3.7's best
173 practices pipeline for SNP calling (McKenna *et al.* 2010), including hard quality filters (Quality by Depth >
174 2.0 & Fisher Strand-bias < 60 & Mapping Quality > 40). The end result was a Variant Call Format (vcf) file
175 containing SNPs for each population. This filtering resulted in a total of 16,674,625 SNPs across all of the
176 *M. sexta* samples on the new assembly (and a similar 16,792,392 for the old assembly).

177 Finally, some inferences of population differentiation relied on differences in allele frequency between
178 locations. For polymorphic sites, estimation of allele frequency depends on inference of which of the
179 alleles (reference or alternate) is ancestral, otherwise allele frequencies are collapsed to the range [0.0,
180 0.5] and information is lost. To infer ancestral state at a given site, variation in *M. sexta* was compared
181 to that in a congener, *Manduca quinquemaculata*. A *Manduca quinquemaculata* sample was sequenced

182 in Mongue *et al.* (2019). Reads from that individual were aligned to the references with Stampy v1.08
183 (Lunter and Goodson 2011), using "--substitutionrate=0.1" to allow for increased single nucleotide
184 mismatches expected from divergences. After initial alignment, this sample was treated in the same
185 manner as the within-species samples (curated with Picard and variants called with GATK), producing
186 9,333,270 high quality single nucleotide variants. These putative divergences were combined with the
187 polymorphism data from *M. sexta* to create a new "ancestral" reference (fasta) for use in polarizing
188 allele frequencies, using the following parsimony logic.

189 In a majority of cases, polymorphic sites did not overlap with divergent sites as well. In other words,
190 these sites that varied in *M. sexta* but not in *M. quinquemaculata* showed the reference allele in the
191 outgroup; thus, the reference allele was taken to be ancestral and left as was. For each site that varied
192 in both *M. sexta* and *M. quinquemaculata*, allele identities were compared between species. If the
193 alternate allele in *M. quinquemaculata* was shared with the alternate allele in *M. sexta* the alternate
194 allele was inferred to be ancestral, and the reference derived. Likewise, if the outgroup was
195 heterozygous at the site, but shared only one allele with the focal species, that allele was inferred to be
196 ancestral (e.g. a tri-allelic site with reference: T, *M. sexta* alternate allele: C, *M. quinquemaculata*
197 alternate alleles: G, C). Considering both of these scenarios, a total of 1,327,986 sites were updated in
198 the reference. In a minority of cases (e.g. a tri-allelic site with reference: T, *M. sexta* alternate allele: C,
199 *M. quinquemaculata* alternate allele: G), there was no most-parsimonious solution. These sites were
200 updated to "N" at the site in the new ancestral reference to mask them from analysis (n = 275,410 sites).
201 The code to generate the updated reference was written in R and can be found in the git repo listed in
202 Data Accessibility.

203 Updating genomic resources

204 In addition to preparation of resequenced samples and variants, the newer reference genome required
205 ancillary metadata, namely: the assignment of scaffolds to chromosomes to separate chromosome-
206 specific effects (e.g. differing dynamics on the Z sex chromosome). Curiously, the newer *M. sexta*
207 reference contains no chromosomal linkage information for its scaffolds. The older assembly does have
208 linkage information however, from previous ortholog counting analyses comparing *M. sexta* to *B. mori*
209 to identify and separate sex-linked scaffolds; this effort generated a chromosome identity for each
210 scaffold, but did not contain information about the ordering of scaffolds within a chromosome (Mongue
211 and Walters 2017). To anchor the newer assembly, it was aligned to the older one using
212 SatsumaSyntenty in Satsuma v.3.1 (Grabherr *et al.* 2010). This tool generated a list of alignments
213 between the older, anchored assembly and the newer, more contiguous but unanchored assembly.
214 Chromosomes were assigned to the new assembly's scaffolds by tabulating the number of fragmented
215 (older) scaffolds aligning to each chromosome-length scaffold and taking the highest scoring
216 chromosome. This effort generated unambiguous assignment of the largest scaffolds in the newer
217 assembly (which should be mostly complete chromosomes) as well as putative assignments for the
218 other, unplaced scaffolds. These placements were mostly unambiguous based on syntenic alignments
219 alone, but in the case of two ambiguities, additional information from BAC-FISH probes between *M.*
220 *sexta* and *B. mori* were used to resolve chromosomal assignment (Yasukochi *et al.* 2009). As this
221 information may be of future use beyond the scope of this research, both this assignment and the
222 alignment summary file used to generate it can be found in the supplementary files.

Population structure

With linkage established, alignments were filtered to separate out the Z chromosome, as unequal sampling of sexes between populations (e.g. North Carolina's sample is male-only) could create spurious patterns. The autosomal genome was used to infer population structure while accounting for uncertainty in genotyping using the software NGSAdmix v. 3.2 (Skotte *et al.* 2013) as well as a principle-component based approach with PCAngsd v.0.98 (Meisner and Albrechtsen 2018). For the admixture analysis, the best-supported number of populations (K) was determined by assessment of ten bootstrapped replicates each for possible K values from 2 to 6, evaluated using the logic from CLUMPAK's web-hosted application (Kopelman *et al.* 2015). After a first round of analyses revealed a large (~8Mb) block of differentiation on chromosome 12 segregating in population, structuring analyses were repeated with this chromosome removed as well.

Characterization of genomic differences

After establishing basic population relationships, population differences were examined in detail. A baseline expectation of differentiation was set by estimating the genome-wide pairwise F_{ST} (excluding the Z chromosome) analyzing the curated alignments with the population genetic software ANGSD v. 0.916 (Korneliussen *et al.* 2014). In more detail, we input into angsd the list of curated bam files and the parsimony-informed ancestral reference sequence and generated site allele frequency likelihoods (-dosaf 1) separately for each population using the SAMtools method of genotype likelihoods (-gl 1). Next, a two-dimensional site frequency spectrum was generated for each pair of populations for a total of three comparisons using the realSFS command. With the relevant site frequency spectrum as a prior, we used the -fstout command to generate genome-wide F_{ST} on using both assemblies as references. Additionally, we estimated F_{ST} separately for silent (four-fold degenerate) and non-silent (zero-fold degenerate) sites to assess whether differentiation skewed toward silent sites or those more likely to be under selection. Identification of zero-fold and four-fold degenerate sites was completed in previous analyses with custom R scripts (in R v 3.3, R Core Team 2017; Mongue *et al.* 2019) but was only carried out on the Kanost et al. assembly due to the higher quality gene models.

With a baseline established, candidates for further investigation were identified via a preliminary scan for F_{ST} outlier regions in windows of 10 kilobases with a 5 Kb step size to identify regions for further study (using the fst command again with -win 10000 -step 5000). All pairwise comparisons were performed: North Carolina (NC) – Arizona (AZ), Kansas (KS) – Arizona, and NC – KS. For these analyses, published chromosome assignments of scaffolds were employed for the older assembly (Kanost *et al.* 2016; Mongue and Walters 2017; Mongue *et al.* 2020) and assignments generated for this manuscript were used for the new assembly. For the older assembly, these assignments did not contain information on ordering of scaffolds *within* a chromosome. Thus, we focused primarily on the new assembly for identification of differentiated regions, but we performed analogous F_{ST} analyses with alignments to the old assembly to assess differentiation in and around coding regions.

These analyses revealed multiple large F_{ST} peaks, as would be expected of segregating inversions. To further investigate these regions and characterize which population(s) carried the ancestral or derived orientation in the putatively inverted regions, genetic diversity was examined as follows. Single nucleotide polymorphism (SNP) frequencies were examined in each population, under the logic that if loci within an inversion cannot freely recombine with the non-inverted orientation, they should share allele frequencies across longer distances than those outside of the inversion. For these analyses the

265 polarized allele frequencies described above were used. SNP variant files (vcfs) were generated for each
266 population and alternate allele frequencies were extracted and examined. Beyond allele frequency, the
267 allele identity was also examined. The VCFtools utility "extract-FORMAT-info GT" (Danecek *et al.* 2011)
268 was used to examine sample genotypes directly and determine which individuals carried non-reference
269 alleles across genetic features of interest. Finally, to further evaluate the interpretation of these regions
270 as inversions, a pair of individuals ostensibly carrying the inversions was investigated with Delly2 v 0.8.7
271 (Rausch *et al.* 2012) to identify structural variants and potential inversion breakpoints. Because Delly
272 makes inferences based on read-pair alignment positions, the individuals with the deepest coverage of
273 those carrying the potential inversions were chosen (A36 and A70) to compare to a pair ostensibly
274 lacking the inversion (S39 and S42).

275 Finally, in the interest of establishing baseline metrics for these populations, we calculated a number of
276 population genetic summary statistics. In particular, we calculated measures of variability: pN
277 (nonsynonymous changes per nonsynonymous site), pS (synonymous changes per synonymous site),
278 pN/pS the scaled ratio of non-synonymous variation, π_0 (variation at zero-fold degenerate sites), π_4
279 (variation at four-fold degenerate sites), Tajima's D_0, and Tajima's D_4 (estimators of deviation from
280 neutral evolution at zero- and four-fold degenerate sites respectively). These metrics were all calculated
281 using alignments to the Kanost et al. assembly for reasons of gene model quality described below.
282 Metrics related to pN/pS relied on SNP calls from the vcf files but estimates of π and Tajima's D were
283 performed directly from alignments using angd's "saf2theta" command. In addition, we calculated ρ^2
284 linkage disequilibrium for non-overlapping 50-basepair windows across the more contiguous Gershman
285 assembly using the vcftools utility "--geno-r2". These results are reported in Table 3 but we refrain from
286 formal statistical comparisons between populations as the uneven sampling effort between them makes
287 estimates of variation difficult to compare directly.

288 Genetic characterization of differentiated regions

289 For each genomic region-of-interest, annotated genes in the region were examined based on the
290 original assembly; this version's annotations have a high degree of manual curation not present in the
291 newer assembly (Kanost *et al.* 2016). *Manduca sexta* has a wealth of available RNA sequence data from
292 both sexes and different life-stages, aggregated as a set of RNAseq collected by Cao and Jiang (2017) and
293 quantified with this older reference. From this dataset, the specificity of gene expression was calculated
294 for each gene in the genome for life-stage, tissue, and sex-specificity (following methods in Mongue,
295 Hansen, & Walters, 2020) to inform potential function of genes-of-interest. More precisely, the
296 specificity metric (SPM) was used to assess the proportion of a given gene's expression found in a
297 specific class. This metric ranges from zero to one, inclusive, and denotes the proportion of a given
298 gene's expression in a focal category (Kryuchkova-Mostacci and Robinson-Rechavi 2017). SPM was
299 calculated for each of the three dimensions of specificity. Stage-specificity was defined as gene
300 expression unique to larva, pupa, or adult *M. sexta* based on a set of tissues collected in all three stages
301 (head, midgut, and fat bodies). Tissue-specificity within a stage was based on tissue types available for
302 that stage (see Table 2). And, naturally, sex-specificity was based on amount of expression unique to
303 males or females. For instance, a gene with an adult SPM of 0.90 shows 90% of its expression in adults
304 as opposed to pupae or larvae. The same gene has separate SPM values that denote how specific its
305 expression is to males or females and which tissues of those individuals. This method has the benefit of
306 generating a sense of gene-function independent of functional annotation based on sequence homology
307 with existing annotations.

All genes across the genome were annotated with SPM values; however, for large outlier regions spanning numerous genes, it was not feasible to examine individual genes in depth. Instead, using the above annotations, these regions were examined for biased composition compared to non-differentiated regions. In other words, enrichment or depletion of functional classes within putative inversions was tested. For small regions containing one or a few genes, each could be manually examined. In these cases, single nucleotide polymorphisms in and around these genes were examined for evidence of coding-sequence variation between populations. SNPs were annotated with the tool SNPeff v. 4.2, which uses gene models to predict the coding sequence changes introduced by polymorphisms (e.g. loss of a canonical stop codon, Cingolani et al., 2012).

Data accessibility

All newly generated sequencing data are available with the following accessions: SRP144217, PRJNA639154 on NCBI. Accessions for RNAseq used in functional inference can be found in (Cao and Jiang 2017). Custom scripts for analysis can be found at github.com/amongue/Manduca_Demography.git. New assembly chromosome assignments can be found in supplementary files.

Results

Chromosomal assignment of the new *M. sexta* assembly

The older, Illumina-only assembly of *M. sexta* already possesses chromosomal assignment based on syntenic alignments to *Bombyx mori*, a well-studied moth in a sister family to *M. sexta*. It has previously been shown that these two species share not only a conserved karyotype (n = 28) but also extensive conservation of sequence along these chromosomes (Yasukochi *et al.* 2009). Initially, we compared synteny between the two assemblies of *M. sexta* to maximize similarity and thus alignment information. From these alignments, 25 of the 28 largest scaffolds in the new assembly matched cleanly and overwhelmingly to one chromosome. The remaining three were more complicated and resolved as follows.

HiC_scaffold_31 showed synteny to both chromosome 2 and chromosome 26, in a way that suggested a potential fusion or misassembly, i.e. the first ~9Mb of the scaffold was syntenic to chromosome 26 and the remaining ~6Mb to chromosome 2. Closer inspection of published BAC-FISH mapping reveals that there has been structural turnover between species and both *B. mori* chr2 and chr26 are orthologous to a fused *M. sexta* chr2 (Yasukochi *et al.* 2009); thus this scaffold was correctly assembled and was manually annotated as chromosome 2.

Second, both HiC_scaffold_2 and HiC_scaffold_25 showed homology to *B. mori* chromosome 11 almost exclusively. Again, the BAC-FISH mapping revealed the reason for the anomaly. Chromosome 11 in *B. mori* is split in *M. sexta* into the larger chromosome 11 and smaller chromosome 26 (Yasukochi *et al.* 2009). Based on the relative sizes of these scaffolds, we annotated the larger (~10Mb) HiC_scaffold_2 as chromosome 11 and the smaller HiC_scaffold_25 (~5Mb) scaffold to chromosome 26.

With these manual annotations, each of the largest 28 scaffolds in the new assembly is now anchored to one of the 28 chromosomes in *M. sexta*. Smaller, more fragmented scaffolds were also assigned to

347 chromosome based on syntenic alignment counts, but without manual curation. These assignments are
348 presented in a supplementary file.

349 Structure

350 We found three populations via the heuristic of Evanno et al. (2005): namely, the most probable K is the
351 one the biggest change in likelihood from the previous K value. Per this metric, each of the three states'
352 moths form distinct populations, although there was some apparent admixture between Arizona and
353 Kansas, including an Arizona individual confidently grouping with the Kansas samples (Figure 2a).

354 Taking a complimentary approach, we assessed principal components of SNP variation across our
355 samples and observed the same clustering pattern as found in the structure analysis. Each state's
356 samples do not cluster with other states, but Arizona samples showing a more dispersed pattern than
357 the others, including some individuals more similar to Kansas individuals than other Arizona individuals
358 (Figure 2b). When excluding chromosome 12, the signal for admixture in some Arizonan moths
359 disappears, and samples all sort by collecting location more cleanly (Figure 2c).

360 Differentiation across the genome

361 To start, we provide population genetic summary statistics for each state in Table 3. Due to the unequal
362 sampling effort between states, we do not formally test for statistical differences between populations.
363 And indeed, absolute values for many measures of variation (e.g. pS or π) are lowest in Kansas, the
364 population with the fewest sampled individuals. Still, the relative amount of non-synonymous variation
365 scaled by synonymous variation (pN/pS) is remarkably consistent across populations, suggesting the
366 strength of selection relative to drift is comparable across states. Moreover, Tajima's D is more negative
367 at zero-fold sites (i.e. those exposed to selection) than four-fold (putatively neutral sites) in each
368 population, which further implies a role for directional selection in each population. Finally, apparent
369 linkage disequilibrium is inversely correlated with sample size, as expected if artificially tight associations
370 are observed between common alleles due to shallower sampling failing to capture rare alleles.

371 A simple genome-wide average of F_{ST} set a baseline level of differentiation of 0.04 to 0.09, depending on
372 the pairwise comparison between states (Table 4). A sliding window scan across the genome revealed a
373 few regions with markedly higher F_{ST} (> 0.5, Figure 3). From this analysis, several regions-of-interest
374 became apparent. Most notably, a large proportion of chromosome 12 shows high levels of
375 differentiation between Arizona and the other two populations. The Z chromosome showed the
376 strongest peak of elevated differentiation, and chromosome 19 showed another above our threshold
377 level. We compared these results on the newer assembly to a parallel F_{ST} scan on the older assembly
378 (Figure S1). As expected, this turned up many differentiated scaffolds assigned to chromosome 12, the Z,
379 and 19, but also 2, 6, and 13. In the following sections we describe each of these regions in detail and
380 resolve apparent discrepancies.

381 An inferred segregating inversion on chromosome 12

382 We observed a large F_{ST} peak across a substantial portion of chromosome 12 in the more contiguous
383 assembly (Figure 4). This peak corresponds with the Delly2 annotation of an inversion located on
384 HiC_scaffold_12 from 5,414,046 Bp to 13,233,866bp, a total of 7.82Mb. Samples from North Carolina
385 annotated with Delly lacked this called inversion, as expected given that the reference individual was
386 sourced from lab stock which was originally collected in North Carolina.

387 In the old assembly, this peak correspond to 13 scaffolds, listed in Table S2 and plotted in Figure S2,
388 summing to 7.6 Mb of sequence, approximately 56% of the total (assigned) length of the chromosome.
389 The peaks contain 321 annotated genes. Note the discrepancy of ~200Kb of differentiated sequence.

390 The putative inversion's frequency of 0.6875 corresponds to 11 of 16 sampled chromosomes with the
391 inversion. Per investigation of sample genotypes, this variation is distributed as 4 individuals
392 homozygous for the non-reference orientation (A36, A70, A78, A82), three heterozygous for it (A71, A76,
393 A84), and one homozygous for the ancestral orientation (A85). Note that the heterozygous individuals
394 correspond to those inferred to be admixed with Kansas and the one homozygous non-inverted
395 individual was grouped with Kansas completely in structure analyses. As discussed above, removing
396 chromosome 12 from structuring analyses leads to less similarity between AZ and KS samples,
397 suggesting the inversion presence/absence is large portion of the signal of the Arizona population. A
398 scan of linkage disequilibrium along the chromosome (Figure S3) showed elevated linkage within the
399 bounds of the hypothesized inversion in each of the three populations, suggesting that this region is a
400 barrier to geneflow between populations.

401 The large size of this inferred inversion (roughly 8Mb and 321 genes contained within) makes identifying
402 a causal adaptive locus challenging. We used the RNA sequencing metadataset to classify genes as
403 specific to one sex (male or female), life stage (larva, pupa, or adult), and tissue (antennae, head,
404 fatbody, midgut, Malpighian tube, muscle, ovaries, or testes) if a given gene showed 70% or more of its
405 expression exclusively in that category. By this metric, the putative inversion on chromosome 12 does
406 not differ in sex-biased composition ($X^2_2 = 1.31$, $p = 0.518$), lifestage-biased composition ($X^2_3 = 2.06$, $p =$
407 0.560), or tissue-biased composition ($X^2_7 = 7.45$, $p = 0.384$) compared to the rest of the genome. Thus,
408 even if there is a set of locally adaptive alleles in this region, it is not one enriched for any of the
409 annotations available to us. Nevertheless, we identified one gene of interest in this region thanks to a
410 misassembly.

411 Both the ostensible chromosome 2 and 13 peaks from the more fragmented assembly belong to the
412 putatively inverted region of chromosome 12 in the newer assembly. The former is rather unremarkable,
413 some 50Kb of a scaffold containing two annotated genes (Msex2.02572 and Msex2.02573) with highly
414 differentiated SNPs localized to areas outside the coding region of either. These variants may be truly
415 neutral or impact the regulation of the nearby genes, but without a better understanding of regulatory
416 elements (e.g. promoter sequences) in this species, it is impossible to say. The peak previously assigned
417 to chromosome 13, deserves more consideration however.

418 A potential pseudogene within the Chromosome 12 inversion

419 Despite overall congruence of results from the old and new assembly, one difference in the F_{ST} scans
420 proved particularly interesting. The older assembly indicated a peak of differentiation on a scaffold
421 anchored to chromosome 13; however, none of the more contiguous chromosome 13 is particularly
422 differentiated using the new assembly as a reference. To reconcile this contradictory pair of results, we
423 investigated the peak in the old assembly first, then placed it in new assembly.

424 This peak comes from one scaffold (scaffold00381) starting around 200Kb and continuing for the
425 remaining 100Kb (Figure 5a). This region contains a single gene, Msex2.10493, and it displays a striking
426 pattern of differentiation between states. Within population variation is low in Kansas and North
427 Carolina, with only 1 and 3 coding-sequence polymorphisms observed, respectively; in contrast, 61 SNPs

428 were called in the gene body from the Arizona samples (summarized in Figure 5b). Moreover, many of
429 these SNPs are at high frequency (Figure 5c), including the predicted loss of a stop codon.

430 The massive difference in called variants theoretically could arise from population-specific differences in
431 mapping rates in this region, either through poor mapping in populations with low SNP counts or (far
432 less likely) a pile-up of reads in Arizona owing to a collapsed segregating paralog. To rule out these
433 artefactual explanations, we examined per-base coverage around this gene and found no differences
434 between populations (Figure 5d; note that slightly deeper coverage in NC is consistent with genome-
435 wide differences in sequencing effort between the populations). Thus, Arizona *M. sexta* appear to truly
436 differ from the other populations with regard to the molecular evolution of this gene, which begs the
437 question of the gene's functional role. Msex2.10493 is overwhelmingly (98.2%) expressed in larvae
438 compared to 1.8% adult expression and vanishingly small pupal expression. Within larvae, this gene
439 shows 97% of its expression in the antennae and another 2.8% in the head.

440 The final question to consider was why such a striking pattern of difference is absent in the newer
441 assembly. To answer this, we examined the syntenic alignment of scaffold00381 to the more contiguous
442 assembly. A discrepancy immediately arose: roughly 2/3^{rds} of the scaffold aligned to HiC_scaffold30
443 (which we have anchored as chromosome 13), but the remaining 1/3rd, including the coding region for
444 Msex2.10493, aligns to chromosome 12 (Supplemental Figure S4). This pattern is suggestive of a
445 misassembly in the older reference genome. Furthermore, the roughly 100Kb length of this apparently
446 chromosome 12 sequence accounts for half of the 200Kb discrepancy in the estimated chromosome 12
447 differentiation peak between the two assemblies.

448 More direct evidence suggests that this potential pseudogene lies within the chromosome 12 inversion.
449 First, the coding sequence of the old assembly's Msex2.10493 is homologous to the new assembly's
450 XM_037442453.1, which lies in the inverted region (roughly 9.257 – 9.261Mb into chromosome 12).
451 Additionally, the frequency of the stop-loss is 0.6875 (= 11/16) and matches that of the most common
452 SNP frequency within the inversion. Moreover, the genotypes (homozygous present, heterozygous,
453 homozygous absent) of the inversion perfectly match the stop-loss variant's genotype. In conclusion,
454 this potential pseudogene sits in the middle of the inferred inversion on chromosome 12, but it was only
455 identified thanks to a serendipitous misassembly in the older version of the *M. sexta* reference.

456 The Z holds another putative segregating inversion

457 The Z chromosome's outliers are attributable to roughly 1Mb in the middle of the chromosome-level
458 scaffold (HiC_scaffold_19). The scale of elevated differentiation suggests another inversion, and our
459 structural variant scan identified an inversion that precisely overlaps this region (from 13,706,400 to
460 14,710,588 bp, for a total length of 1,004,188 bp). Further evidence for a lack of recombination in this
461 region can be seen in the non-reference allele frequencies which vary across the scaffold in both NC and
462 AZ but show a tract of SNPs with a common frequency of 0.93 (= 13/14) within the putative inverted
463 region in Arizona (Figure 6).

464 This peak of differentiation is also identifiable in the older assembly as a roughly 1Mb region of
465 scaffold00022, suggesting we are capturing essentially all of the inversion on one scaffold, even in the
466 more fragmented assembly, (Figure S5). In terms of gene content, scaffold00022 contains 35 genes and
467 shows an significant excess of unbiased genes (i.e. those expressed in both sexes, X^2_2 = 11.36, p =

468 0.0034), compared to the rest of the Z, which is significantly masculinized, as previously reported
469 (Mongue *et al.* 2020).

470 Chromosomes 6 and 19 show differentiation but no clearly differentiated genes

471 Chromosome 6 shows a single peak of divergence, though this region is only weakly differentiated,
472 barely meeting our cut-off threshold for exploration (F_{ST} > 0.5 between any two populations). This region
473 contains three full annotated genes (Msex2.12148, Msex2.12149, and Msex2.12150), but no SNPs
474 within coding regions.

475 Two outlier scaffolds in the older assembly localize to chromosome 19; both represent differentiation
476 between Arizona and the other two states. In the newer, more contiguous assembly, these peaks
477 remain distinct from each other (Figure S6), suggesting they are not parts of a common feature. One is
478 localized to scaffold00118, to approximately the last 400Kb of an ~850Kb scaffold. This region contains
479 11 annotated genes (Msex2.05775-Msex2.05786), but none of these shows skews in coding region SNPs
480 between populations as extreme as seen on the potential pseudogene mentioned above. However, two
481 genes do show more modest deviation between states. Msex2.05777 is variable in both North Carolina
482 (Pn = 6, Ps = 10) and Kansas (Pn = 7, Ps = 12) but monomorphic (Pn = 0, Ps = 0) in Arizona. Conversely,
483 Msex2.05784 is non-variable in the North Carolina and Kansas samples but contains 3 non-synonymous
484 variants and 1 synonymous variant in Arizona.

485 The second peak, on scaffold00419, seems to span the length of this 200Kb scaffold, but this may reflect
486 the limits of resolution of our F_{ST} window-size. In any case, the entire scaffold contains 11 annotated
487 genes, many of which have no expression data and no called SNPs in any population. As such, we do not
488 place much emphasis on the differentiation around these dubiously annotated regions.

489 Discussion

490 We conducted whole genome resequencing to investigate the natural variation of *Manduca sexta*
491 populations across the United States. In brief, we found that individuals from three populations across
492 an East-West transect are genetically differentiated. This result may not seem surprising, but studies of
493 other Lepidoptera have at times found evidence for continent-wide panmixis (specifically for monarch
494 butterflies, Lyons et al., 2012; Zhan et al., 2014). And while monarchs may be an extreme case of
495 lepidopteran long-distance travel, sphinx moths, including *M. sexta*, are renowned for their flight and
496 dispersal ability, both in terms of small-scale speed and dexterity (Stevenson *et al.* 1995) and long-
497 distance dispersal (Janzen 1984; Haber and Frankie 1989). Indeed, *M. sexta* has been posited as
498 migratory in the past (Ferguson 1991). Our results, however, suggest that gene flow is less common than
499 expected of a species with routine migration. In fact, the genome-wide mean F_{ST} for the least
500 differentiated pair (0.04, Kansas-Arizona) is on par with the differentiation between migratory North
501 American monarchs and the Hawaiian population that is thought to have split roughly 200 years ago
502 (Lyons *et al.* 2012).

503 More striking than this level of differentiation is the nature of the differences that contribute to it.
504 Namely, large (>1 Mb) putative inversions, are key contributors to the variation between populations.
505 Sustained tracts of differentiation are most apparent on two chromosomes, the Z chromosome and
506 chromosome 12. In both cases, the Arizona population is distinct from Kansas and North Carolina. We
507 note that the smaller sample size of Kansas *M. sexta* decreases the precision of allele frequency

508 estimation (Lou *et al.* 2020), and may obscure some of the more subtle population differences for the
509 time being. For the present study, we discuss in detail the genomic and genetic nature of the large
510 differences, with the caveat that functional genetics will be required to truly confirm the genomic
511 structure and downstream fitness consequences of this variation.

512 The largest signal for population differentiation: a likely inversion on chromosome 12

513 A long tract of chromosome 12 showed high levels of differentiation in our F_{ST} scan. This signal belonged
514 to a single block of sequence, spanning 8 megabases (roughly half the length of the chromosome),
515 containing over 300 annotated genes, and found at a frequency of almost 70% in the Arizona population.
516 Individuals that are heterozygous for this putative inversion or lacking it entirely cluster more closely
517 with the Kansas population than other Arizona samples which are homozygous for it. When removing
518 chromosome 12 from analyses, all Arizona samples cluster more closely with each other than with
519 Kansas however, suggesting that the two populations are differentiated across the genome, but that the
520 sheer number of variants associated with the putative inversion swamps other signals. These two
521 observations combine to suggest that the inversion has been segregating in the population for some
522 time.

523 In general, and especially in large populations, inversion frequencies are thought to imply something
524 about their selective effects, with only beneficial variants reaching high frequency (Lande 1984;
525 Kirkpatrick and Barton 2006). In other species in which naturally occurring inversions have been studied,
526 this expectation has been borne out. Low frequency inversions (e.g. 8%) are associated with fitness
527 tradeoffs (Lee *et al.* 2016) and more common inversions (~50%) may have little to no fitness costs (Knief
528 *et al.* 2016), at least locally. Their absence elsewhere may suggest a lack of gene flow or that there *are*
529 fitness costs in other environmental backgrounds. Indeed, linkage disequilibrium is higher within the
530 bounds of the inverted region even in populations in which we did not detect the variant, suggesting a
531 dampening of gene flow between populations here. From this perspective, the common chromosome
532 12 variant seems likely to be at least selectively neutral, if not beneficial, in Arizona. However, the large
533 number of encompassed genes present a challenge for identifying selectively relevant loci from purely
534 computational methods. Still, one gene-of-interest arose from our efforts to cross-check results with the
535 older *M. sexta* reference (Kanost *et al.* 2016).

536 A likely candidate for local adaptation in the inversion: an apparent pseudogene

537 An F_{ST} scan of the older assembly with the same resequencing data revealed numerous outlier scaffolds
538 anchored to chromosome 12 as expected. However, an additional similar peak was detected on a
539 scaffold assigned to chromosome 13. Alternate allele frequencies on this peak matched those most
540 commonly seen in the chromosome 12 inversion, and a closer inspection of synteny between the old
541 and new assemblies suggested that this scaffold is likely a chimera. The majority of sequence belongs to
542 chromosome 13, but the differentiated region is syntenic to chromosome 12 within the inversion. This
543 region contains a single annotated gene, Msex2.10493 (in the old annotation; XM_037442453.1 in the
544 new annotation). It carries almost no variation in North Carolina or Kansas but has a wealth of high
545 frequency variants (61 SNPs in our sample) in the Arizona population, one of which is a predicted stop-
546 loss in the coding region. A large-effect SNP like this could easily break the protein function via
547 translation of otherwise non-coding DNA. While inconclusive from molecular data alone, a hypothetical
548 loss of function would easily explain the preponderance of SNPs found in Arizona; pseudogenization
549 instantly relaxes selective pressure such that subsequent variants can accrue quickly. And indeed, the

high frequency of this stop-loss suggests that it cannot have an appreciable fitness cost, or it would not have persisted in the population. Naturally, this raises the question of what function this gene has that it could be lost without strong selective consequences. Or, alternatively, could a loss of function be adaptive under certain circumstances?

Based on our expression characterization, the Msex2.10493 gene is almost exclusively expressed in larval antennae, which are known to play a role in olfaction and food choice in *M. sexta* (Boer and Hanson 1987). Olfaction genes are among the most commonly observed to pseudogenize in other species, ostensibly because the fitness consequences of their loss are rarely lethal (Nei *et al.* 2008; Prieto-Godino *et al.* 2016). Intriguingly, while most populations of *M. sexta* feed almost exclusively on plants in the family Solanaceae, larval Arizona hornworms have been recorded eating the unrelated devil's claw (Martyniaceae: *Proboscidea parviflora*, Mechaber & Hildebrand, 2000). It is tempting to make the connection between the apparent loss of function of a larval sensory gene and the exploitation of a new hostplant, as research on the silkmoth (*B. mori*) has shown that knockout of a single chemoreceptor is sufficient to turn naturally specialist larvae into generalists (Zhang *et al.* 2019); however, it will take further study to establish whether or not a similar situation is occurring in *M. sexta.*

Still, the placement of this apparent pseudogene within a massive block of elevated differentiation between populations and its potential relationship with hostplant ecology is suggestive of a locally adapting region. As genomic scans of natural variation become more common, so too does the observation that many species harbor regions of large-scale differentiation that distinguish individuals adapted to different environments (Fuller *et al.* 2019; Todesco *et al.* 2020; Mérot *et al.* 2021, 2021). In such instances, suppressed recombination, typically through inversions, keep locally beneficial alleles from being decoupled from each other, even in the face of gene flow from other populations. The frequencies of these large variants typically follow an environmental (or more directly a selective) cline (Kapun *et al.* 2016; Wellenreuther *et al.* 2017). We do not have the geographic resolution to detect any potential cline in the frequency of this inversion and pseudogene, but presence and absence data are at least consistent with a role in expanded hostplant usage.

The devil's claw plant's native range is limited to the desert southwest of North America (particularly: northern Mexico and California, Arizona, New Mexico, Utah, and Nevada in the United States; see Berry *et al.* 1981). As expected based on this range, we did not observe any *M. sexta* carrying the putative inversion in North Carolina or Kansas. With only four sampled individuals from Kansas, we cannot exclude the possibility that the Arizona inversion is present there as well, albeit at a much lower frequency, but to follow the logic of the devil's claw hypothesis, there would be no local benefit for individuals carrying the pseudogene outside of the southwest. Indeed, in the absence of a novel hostplant with the correct set of complex phytochemistry, becoming less choosy could be maladaptive. Zhang et al. (2019) found that although chemoreceptor-knockout silkworms readily ate many food sources, they failed to finish development and pupation on all but the traditional hostplant. To reiterate, these inferences are highly speculative, but they create easily testable hypotheses. Laboratory studies of Arizonan *M. sexta* with the putative inversion and pseudogene will be needed to unpack the functional consequences of this striking variation.

A Z inversion in AZ: a role for sex-bias driving rearrangement

The single highest peak of differentiation in our genome-wide scan comes from the Z chromosome. This region, with roughly 1 Mb of extended differentiation and shared allele frequencies in Arizona also fits

592 the pattern of a segregating inversion between populations. Moreover, the non-reference orientation is
593 nearly fixed in the Southwest population, being homozygous (or present in hemizygous females) in all
594 but one individual. As discussed above, an inversion is unlikely to reach such high frequency without
595 some selective advantage.

596 Here, even without specific gene functional annotations, we have a reasonable hypothesis for what
597 could drive this structural variant to near-fixation. We found that the inversion contains a significant
598 excess of genes expressed in both sexes (i.e. unbiased genes), compared to the rest of the Z
599 chromosome, which is male-biased (Mongue and Walters 2017). As has been recently shown, unbiased
600 genes are an important source of positive selection on the Z in *M. sexta* (Mongue *et al.* 2021). These
601 genes are expressed in a haploid state in females (which have only one Z chromosome); thus, even
602 recessive beneficial mutations are exposed to positive selection (Rice 1984; Charlesworth *et al.* 1987).
603 The capture of positively selected variants of such genes in a non-recombining region would ensure their
604 co-transmission and seems a reasonable explanation for this inversion's prevalence.

605 Moreover, these sex chromosome dynamics intersect with the population genetics of local adaptation in
606 synergistic ways. Modeling suggests that the exposure of recessive alleles to selection should facilitate
607 local adaptation and make the sex chromosomes hotspots for this phenomenon (Lasne *et al.* 2017). For
608 similar reasons, sex-linked inversions are thought to sweep to fixation more easily than autosomal
609 inversions (Connallon *et al.* 2018). As such, it is unsurprising to find the Z involved in short-term
610 differentiation as well as long term adaptation (Mongue *et al.* 2021) in this species.

611 Other differentiated regions of the genome

612 The inversions discussed above are the most apparent sources of regional differentiation, but
613 chromosomes 6 and 19 also showed elevations in differentiation at smaller scales. For the most part,
614 differentiated regions fell outside of coding regions or near dubiously annotated genes (i.e. those not
615 supported by expression data). Lacking further information for hypothesized importance, they are not
616 discussed in detail here for brevity's sake.

617 Conclusions

618 We report that *M. sexta* from Arizona, Kansas, and North Carolina are genetically differentiated. The
619 confirmation of regional differentiation is a valuable addition to research in both laboratory and field
620 studies, as well as to development of management plans for this crop pest between regions. That said,
621 we have yet to establish the minimum geographic scale at which *M. sexta* populations are structured
622 (for instance how much gene flow exists between adjacent states or even within a single state). This
623 finer scale sampling will be particularly important for agricultural centers on the applied side, and
624 additional sampling will also provide more insight into the large-scale variation we report here.

625 At least two large inversions and a potential pseudogene differentiate Arizona from the Kansas and
626 North Carolina populations. All of these variants are high frequency (> 0.5) within Arizona but absent in
627 the other populations. However, the nature of our sample collection limits the inferences we can make
628 at present. For instance, the high frequency of the variants suggests they are not deleterious, but with
629 only a single time-point of sampling in Arizona, it is hard to say whether or not these variants have
630 reached an equilibrium frequency. Additionally, other studies have shown inversion polymorphisms to
631 follow geographic or environmental clines (Anderson *et al.* 2005; Wellenreuther *et al.* 2017). In such
632 cases, the inversions often hold locally adaptive alleles that are maintained in spatial polymorphism by

differences in environmental factors, but for *M. sexta*, with each sampled state separated from the others by at least 1,500 kilometers, it is impossible to say if these segregating variants also follow a cline in the region or to which climactic variables they may relate. Additional sampling of the Southwest will be required to assess how widespread the inversions are.

Likewise, controlled laboratory studies will be required to assess the fitness consequences of the segregating stop-loss in a larval antennal gene within the chromosome 12 inversion. In particular, the coincidence of a novel larval hostplant in Arizona and a large-effect mutation in a gene expressed in a larval chemosensory gene are suggestive but far from conclusive. The relationship between the two will require hostplant choice experiments for larvae with and without the stop-loss mutation.

Finally, it is worth noting that these dramatic differences between populations could not be observed in standard lab strains, which are all derived from the North Carolina population to our knowledge. On the other hand, without extensive lab studies and RNA-sequencing, we would not have the information to form functional hypotheses for these variants found in wild populations. Beyond the immediate utility of these data, the results we present here serve as a reminder of the efficacy of integrating laboratory and field research within the same study system.

Acknowledgements

This project was partially funded by NSF DDIG to AJM (DEB-1701931) and DEB #1557007 and IOS #1920895 to AYK. The authors wish to acknowledge Wesley Mason and Michael Hulet and the rest of the Information and Telecommunication Technology Center (ITTC) staff at the University of Kansas for their support with our high-performance computing. The authors also thank the University of Kansas's Entomology Endowment for additional funding support in sequencing. Thanks to Paul Hime for guidance on population structure analysis. Thank you to Clyde Sorenson, Judie Bronstein, and Goggy Davidowitz, for initial and continued support in investigating population genomics of *M. sexta*. Kelly Dexter and Rebecca Messcher helped provide the samples from University of Florida's McGuire Center collection. Thanks also to the members of Ashworth 2.02 for continued patience in the discussion of the material of this manuscript.

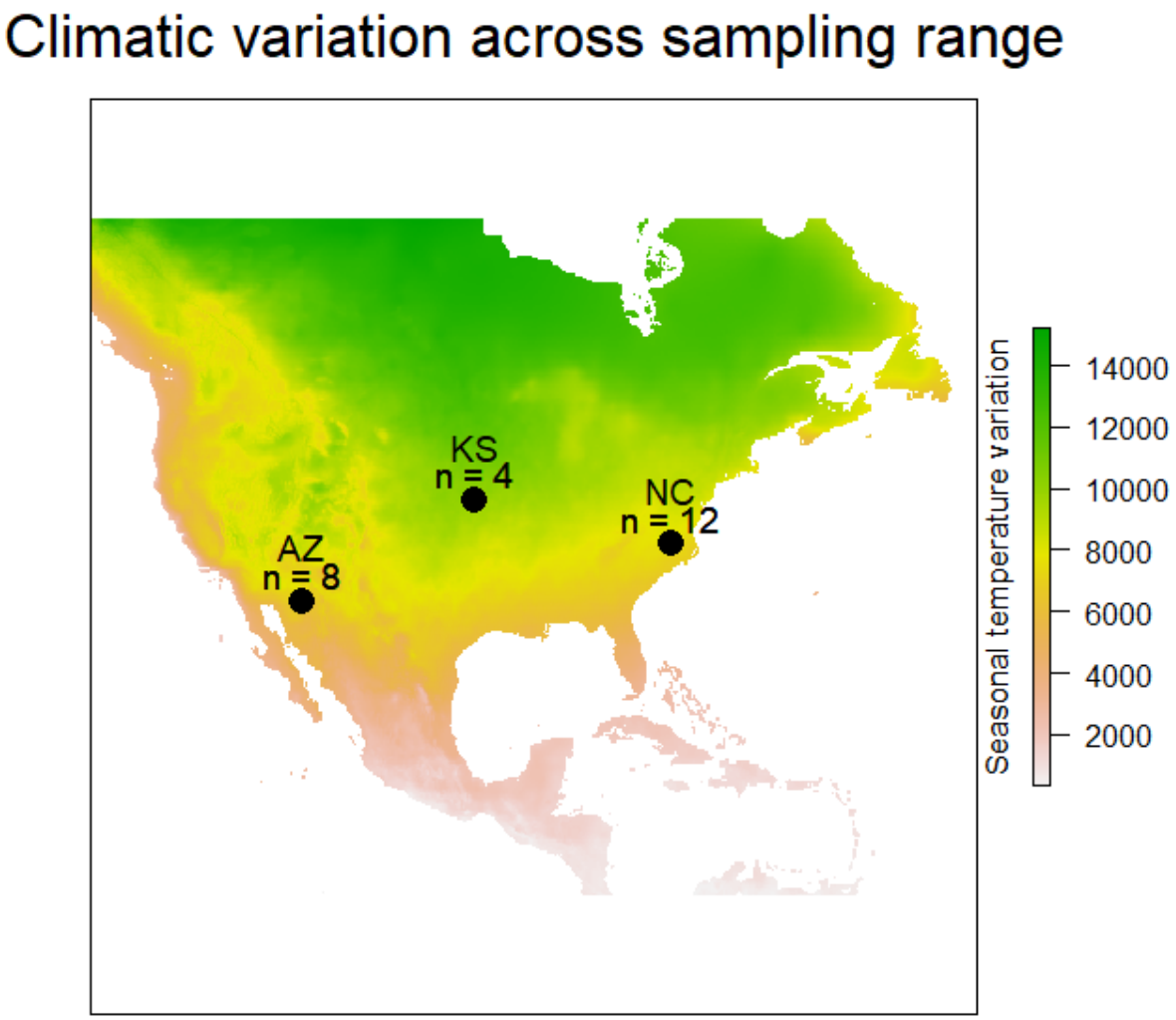

Figure 1. Location of sampled populations of tobacco hornworms with sample sizes. From left to right: Arizona (AZ), Kansas (KS), and North Carolina (NC). Locations are plotted against a backdrop of temperature seasonality (the annual standard deviation in average monthly temperature) to demonstrate that local environment varies across the range of the species.

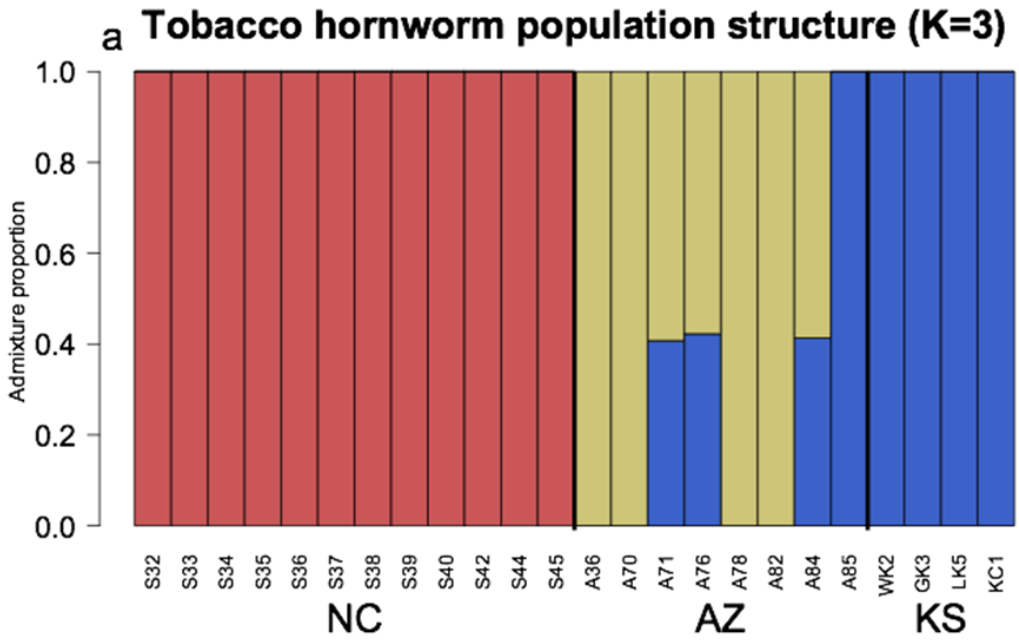
a
Tobacco hornworm population structure (K=3)
Admixture proportion
1.0
0.8
0.6
0.4
0.2
0.0
S32
S33
S34
S35
S36
S37
S38
S39
S40
S42
S44
S45
A36
A70
A71
A76
A78
A82
A84
A85
WK2
GK3
LK5
KC1
NC
AZ
KS

671

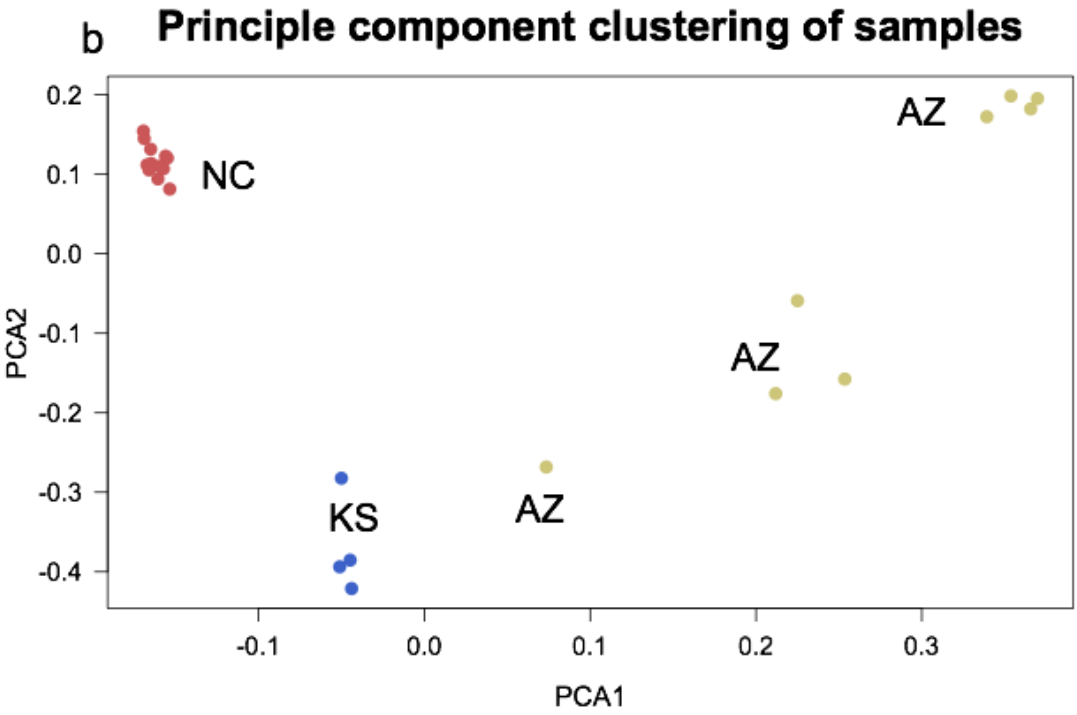
b
Principle component clustering of samples
PCA2
0.2
0.1
0.0
-0.1
-0.2
-0.3
-0.4
NC
AZ
AZ
KS
AZ
-0.1
0.0
0.1
0.2
0.3
PCA1

672

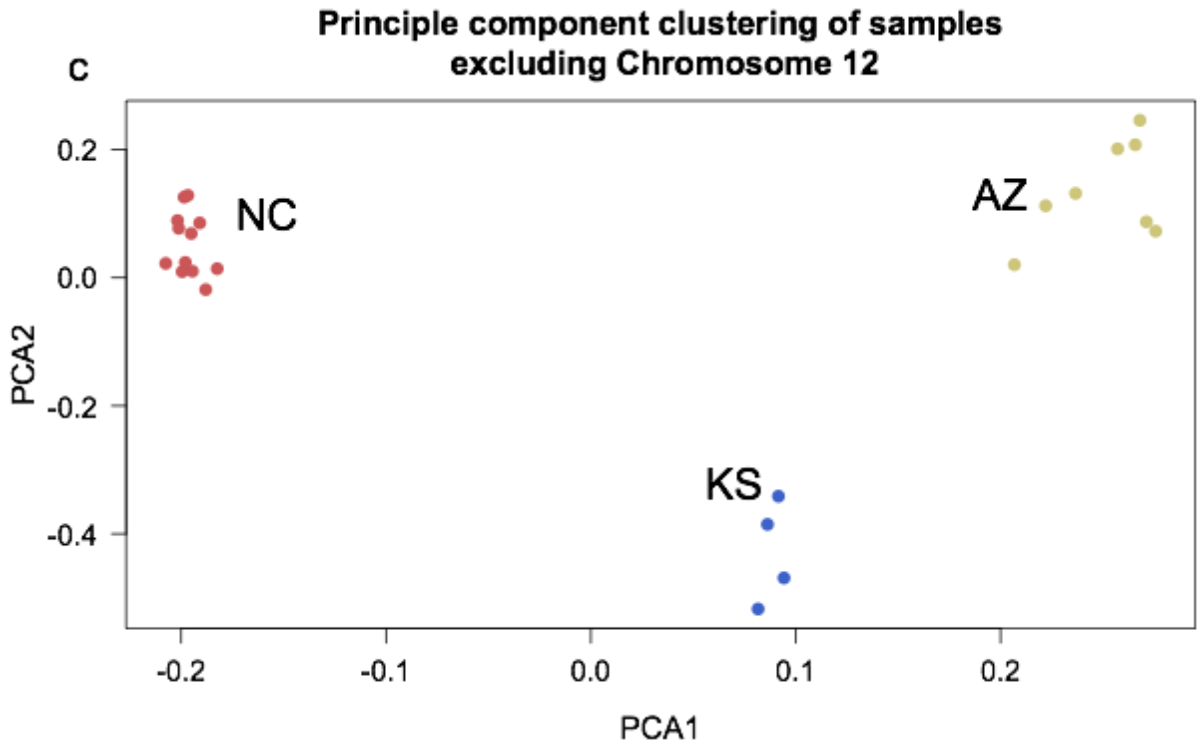

673

674 **Figure 2.** Population structure of *M. sexta* based on whole-genome resequencing of North Carolina (NC),
675 Arizona (AZ), and Kansas (KS) individuals, omitting the Z chromosome. **(a)** Clustering of samples based
676 on the most likely K (3), demonstrating that moths from different states are genetically differentiable.
677 **(b)** Principle component analysis of the same dataset, with coloring the same as in (a). Note in both
678 cases that Arizona individual (A85) clusters more closely with Kansas than other Arizona samples and
679 three others (A71, A76, and A84) fall in between Kansas and the other four Arizona samples. Additional
680 analysis revealed that these individuals lacked a large chromosome 12 inversion unique to the AZ
681 population. **(c)** Excluding this chromosome from analysis causes all AZ individuals to cluster more closely
682 with each other than with KS.

683

684

685

686

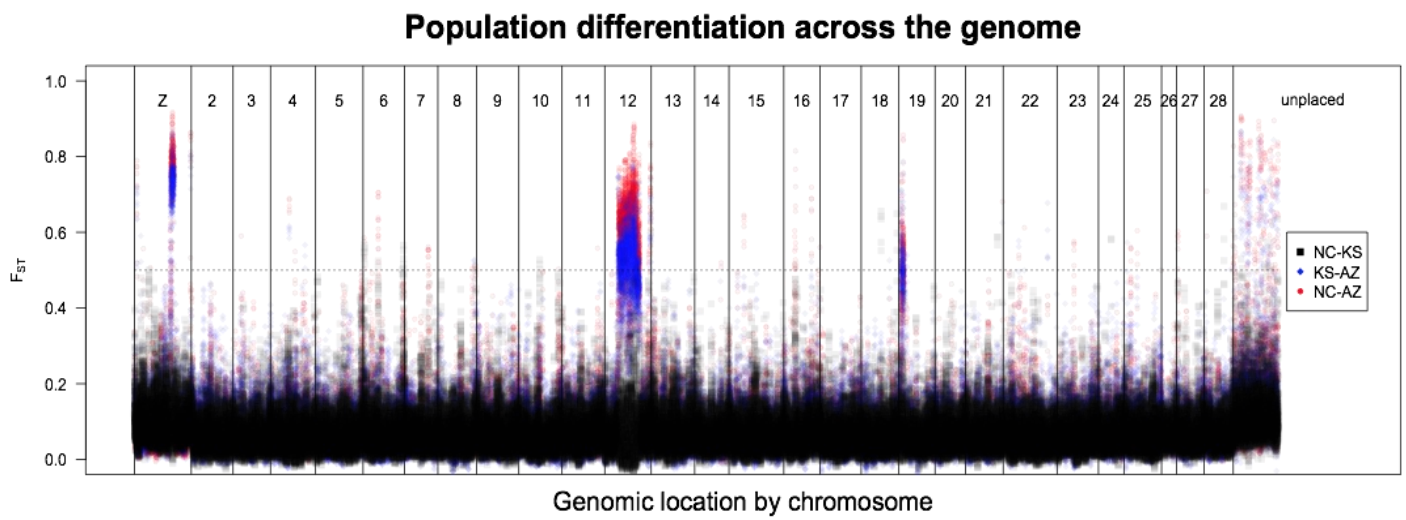

Figure 3. Pairwise differentiation (F_{ST}) across the *M. sexta* genome: North Carolina (NC) vs. Kansas (KS; black squares), Kansas vs. Arizona (AZ; blue diamonds), and North Carolina vs. Arizona (red points). Plotting is ordered by chromosomal linkage, but not ordered within a chromosome. We examined regions enriched for differentiation greater than 0.5 (dashed line). By this metric, one peak on the Z, and one peak each on chromosomes 12 and 19. Additionally, note that the highest peaks almost always come from KS vs. AZ and NC vs. AZ, indicating that Arizona's population is more distinct from the others than NC and KS are from each other. Chromosomes are numbered based on syntenic assignment of HiC scaffolds from the Gershman assembly. Unplace scaffolds are all those beyond the 28 main chromosomal scaffolds.

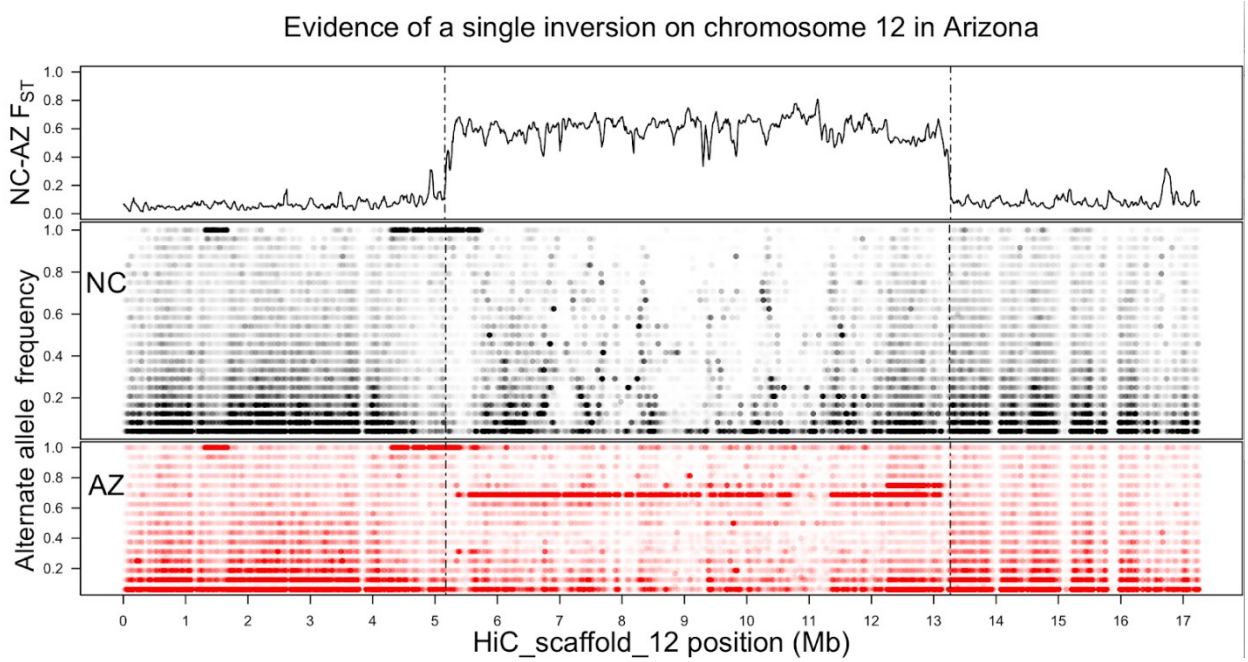

Figure 4. Evidence of a single segregating inversion on chromosome 12 from the newly released *M. sexta* assembly (Gershman *et al.* 2021). **Top.** F_{ST} comparison for the North Carolina and Arizona populations shows a roughly 8 Mb region (between 5.3-13.3 Mb) of elevated differentiation between the populations, corresponding to the length of the two tracts of differentiation from Figure 3, plus some additional unplaced peaks. Vertical dashed lines delimit this differentiated region and extend below for ease of comparison between populations. **Middle and Bottom.** Frequencies of alternate alleles for called SNPs in North Carolina (middle) and Arizona (bottom). Points are semi-transparent such that opaquer regions are denser with variants. Arizona appears to hold the inverted orientation as a single allele frequency (0.6875 or 11/16) dominates the differentiated region, whereas North Carolinian allele frequencies are variable throughout. Also in the 1-2 Mb and 4-5 Mb regions are areas of dense SNPs fixed in both populations. These are interpreted as regions in which the lab strain used to generate the reference has differentiated from the wild populations.

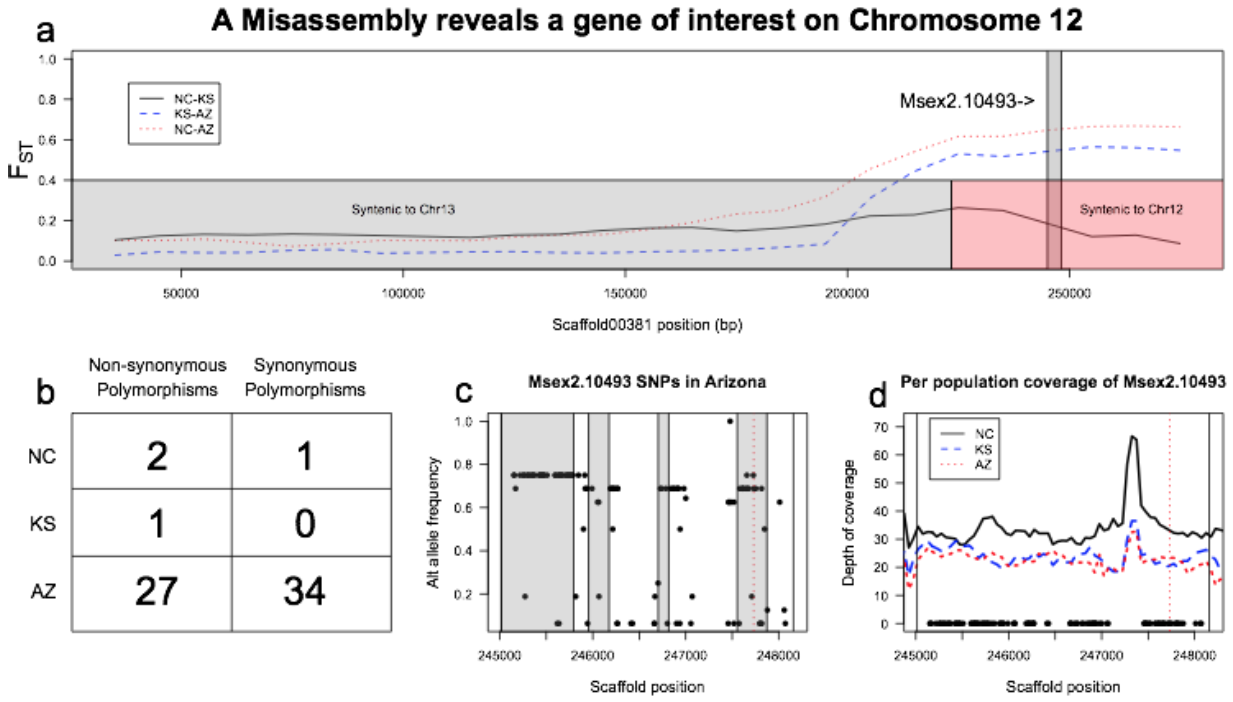

Figure 5. Extreme population differentiation of a gene within chromosome 12's putative inversion. **a.** Finer scale plotting of F_{ST} of the differentiated Kanost et al. scaffold, previously assigned to chromosome 13 shows that differentiation occurs beyond 200 Kb and, as with the inversions above, it appears that Arizona is markedly different from North Carolina and Kansas. Boxes at the bottom of the plot show syntenic alignments with the Gershman et al. assemble and reveal that the differentiated region belongs to chromosome 12 rather than 12. A single annotated gene, Msex2.10493, lies in this region (grey box). **b.** Annotation of SNPs in the coding region reveals a stark difference in variation between populations. Arizona moths hold more than ten times the non-synonymous polymorphisms than those in the other two states. **c.** Frequencies of the SNPs in Arizona. Grey boxes represent exons and the dashed vertical line marks a variant that disrupts the annotated stop codon. **d.** Depth of coverage of the gene in question does not vary between populations in a way that suggests differences in alignment between populations can explain the differences in called SNPs.

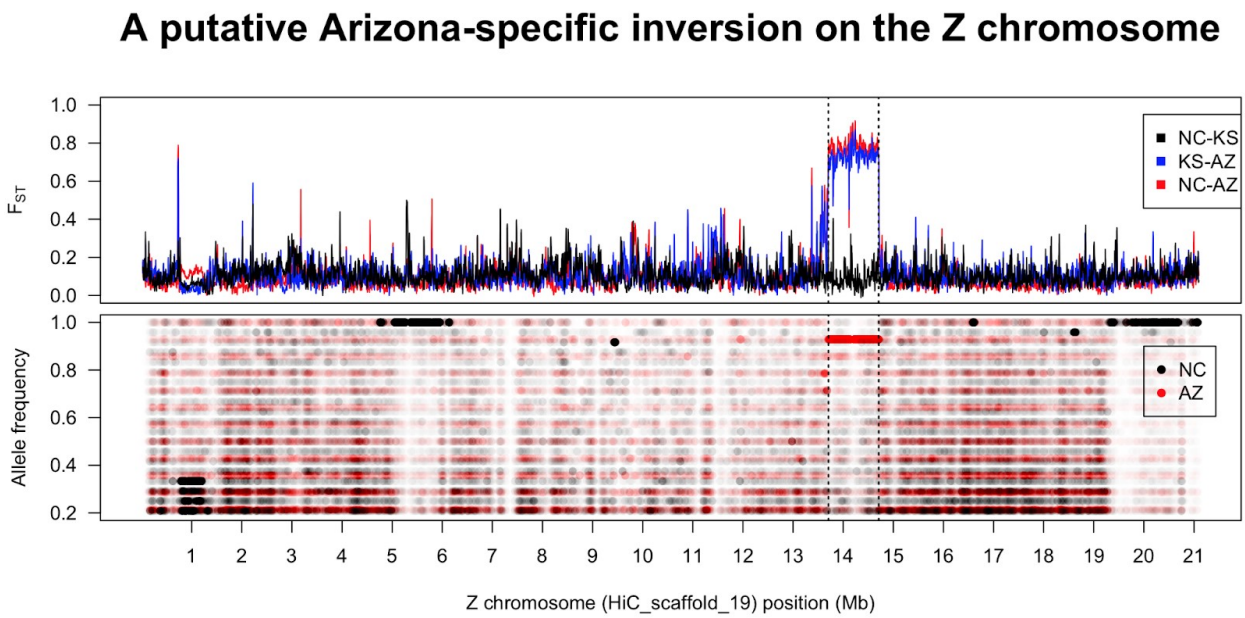

Figure 6. Evidence for an inversion on the Z chromosome. **Top.** A roughly 1 Mb portion of the Z shows elevated differentiation in North Carolina – Arizona and Kansas – Arizona comparisons. Here, as well as below, this region corresponds to an inversion identified by Delly2 (from 13.7 to 14.7 Mb.). **Bottom.** Like the chromosome 12 inversion, Arizona shows a long tract of shared non-reference allele frequencies in the region while North Carolina does not (note that Kansas allele frequencies are omitted due to lower sampling effort artificially stratifying frequencies). Inferred blocks of non-reference SNPs that do not correspond to similar F_{ST} peaks are inferred to be regions in which the lab-strain used for sequencing has differentiated from the natural populations.

Sample	State	Location	Collecting method	Sex	Overall alignment rate (bowtie2 vsl)	Coverage depth (x)
A36	AZ	Madera Canyon	Blacklight trapped adult	M	94.08%	18
A70	AZ	Madera Canyon	Blacklight trapped adult	M*	94.13%	18
A71	AZ	Madera Canyon	Blacklight trapped adult	F*	93.60%	17.8
A76	AZ	Madera Canyon	Blacklight trapped adult	F	93.61%	13.7
A78	AZ	Madera Canyon	Blacklight trapped adult	M	94.00%	14.7
A82	AZ	Madera Canyon	Blacklight trapped adult	M	94.09%	14.5
A84	AZ	Madera Canyon	Blacklight trapped adult	M	94.18%	14.2
A85	AZ	Madera Canyon	Blacklight trapped adult	M	94.20%	14
WK2	KS	Williamstown	Larva from hostplant	F	93.65%	14.5
KC1	KS	Kansas City	Larva from hostplant	F	93.77%	15.9
LK5	KS	Lawrence	Larva from hostplant	F	94.04%	16.2
GK3	KS	Garnett	Larva from hostplant	M	94.55%	18
S32	NC	Rocky Mount	Blacklight trapped adult	M	94.12%	18.13
S33	NC	Rocky Mount	Blacklight trapped adult	M	93.90%	19.82
S34	NC	Rocky Mount	Blacklight trapped adult	M	93.84%	18.90
S35	NC	Rocky Mount	Blacklight trapped adult	M	94.02%	16.93
S36	NC	Rocky Mount	Blacklight trapped adult	M	94.04%	19.13
S37	NC	Rocky Mount	Blacklight trapped	M	94.06%	20.08

			adult			
S38	NC	Rocky Mount	Blacklight trapped adult	M	94.08%	22.44
S39	NC	Rocky Mount	Blacklight trapped adult	M	94.01%	26.16
S40	NC	Rocky Mount	Blacklight trapped adult	M	93.79%	19.72
S42	NC	Rocky Mount	Blacklight trapped adult	M	94.12%	25.67
S44	NC	Rocky Mount	Blacklight trapped adult	M	94.07%	22.10
S45	NC	Rocky Mount	Blacklight trapped adult	M	94.16%	20.49
Q6	NC	Rocky Mount	Blacklight trapped adult	M	85.44%	11.2

Table 1. Sample collection and alignment information. Sample names follow sample labeling in SRA. States are abbreviated as AZ (Arizona), KS (Kansas), and NC (North Carolina). Basic genomic information on overall alignment rates to the published *M. sexta* genome (Kanost *et al.* 2016) and depth of sequencing coverage are given as well. All sequencing data are available with the following accessions: SRP144217, PRJNA639154 on NCBI. Individuals with an * next to their sex did not have sex information recorded during sampling; however, we were still able to assign sex based on coverage ratios between the Z chromosome and autosome after sequencing. Q6 is the *M. quinquemaculata* sample used as an outgroup to polarize allele frequencies.

	Antenna		Head	Muscle	Midgut	Malpighian tubes	Fat	Gonad	
Larva									
Pupa								M	F
Adult	M	F						M	F

Table 2. Tissue-specific RNA sequencing available for each life-stage of *M. sexta*. This dataset forms the basis for tissue specificity labeling annotation of genes in this study. Grey cells indicate presence, empty cells denote absence of data. If sex specific data are available, it is noted with an M (for male) and F (female) in the relevant cell. For larvae, few tissues were sampled at multiple instars, so no further developmental division was made.

Table 3. Population genetic parameters across the autosomes of the populations surveyed here. The Z chromosome was omitted due to uneven sampling of sexes between populations. Median values are given for polymorphism estimates (to avoid skew from outliers), while means are reported for Tajima's D (as in every case, the median value is centered on zero). For all statistics involving silent and replacement sites (i.e. everything but linkage) the older Kanost et al. assembly was used to take advantage of higher confidence gene models. Mean linkage disequilibrium (ρ^2) reported for 50 basepair windows using the Gershman et al. assembly to take advantage of more robustly supported linkage groups. Standard deviations appear in parentheses.

	Population genetic summary statistics for each population surveyed		
	North Carolina	Kansas	Arizona
pN	0.0068 (±0.022)	0.0044 (±0.0198)	0.0063 (±0.027)
pS	0.0232 (±0.050)	0.0140 (±0.050)	0.0197 (±0.058)
pN/pS	0.2850 (±0.656)	0.2852 (±0.665)	0.2851 (±0.652)
π_0	$8.82*10^{-9}$ (±0.030)	$4.27*10^{-8}$ (±0.034)	$7.95*10^{-8}$ (±0.032)
π_4	$5.96*10^{-8}$ (±0.082)	$3.37*10^{-7}$ (±0.090)	$4.32*10^{-7}$ (±0.086)
Tajima's D_0	-0.0795 (±0.433)	-0.0367 (±0.299)	-0.0673 (±0.354)
Tajima's D_4	-0.0259 (±0.510)	-0.0148 (±0.368)	-0.0259 (±0.406)
ρ^2	0.3538 (±0.396)	0.5990 (±0.392)	0.4053 (±0.401)

F_{ST} 0x, 4x	**NC**	**KS**
KS	0.064, 0.054	
AZ	0.090, 0.081	0.041, 0.044

Table 4. Genome-wide point estimates (excluding the Z chromosome) for differentiation between each pairwise combination of the three populations studied here. In each comparison differentiation at sites exposed to selection (i.e. zero-fold degenerate sites, 0x) and putatively neutral sites (four-fold degenerate sites, 4x) were estimated separately in angsd using the gene models from the Kanost et al. assembly.

816

817

818

819

820 ## References

821 Anderson, A. R., A. A. Hoffmann, S. W. McKechnie, P. A. Umina, and A. R. Weeks, 2005 The latitudinal
822 cline in the In (3R) Payne inversion polymorphism has shifted in the last 20 years in Australian
823 Drosophila melanogaster populations. Molecular Ecology 14: 851–858.
824 Banister, M. J., and R. H. White, 1987 Pigment migration in the compound eye of Manduca sexta: effects
825 of light, nitrogen and carbon dioxide. Journal of insect physiology 33: 733–743.
826 Berry, J., P. Bretting, G. Nabhan, and C. Weber, 1981 Domesticated Proboscidea parviflora: a potential
827 oilseed crop for arid lands. Journal of Arid Environments 4: 147–160.
828 Boer, G. de, and F. E. Hanson, 1987 Differentiation of roles of chemosensory organs in food
829 discrimination among host and non-host plants by larvae of the tobacco hornworm, Manduca
830 sexta. Physiological Entomology 12: 387–398.
831 Cao, X., and H. Jiang, 2017 An analysis of 67 RNA-seq datasets from various tissues at different stages of
832 a model insect, *Manduca sexta*. BMC Genomics 18:.
833 Charlesworth, B., J. A. Coyne, and N. H. Barton, 1987 The relative rates of evolution of sex chromosomes
834 and autosomes. The American Naturalist 130: 113–146.
835 Cingolani, P., A. Platts, L. L. Wang, M. Coon, T. Nguyen *et al.*, 2012 A program for annotating and
836 predicting the effects of single nucleotide polymorphisms, SnpEff: SNPs in the genome of
837 *Drosophila melanogaster* strain w 1118; iso-2; iso-3. Fly 6: 80–92.
838 Connallon, T., C. Olito, L. Dutoit, H. Papoli, F. Ruzicka *et al.*, 2018 Local adaptation and the evolution of
839 inversions on sex chromosomes and autosomes. Philosophical Transactions of the Royal Society
840 B: Biological Sciences 373: 20170423.
841 Contreras, H. L., J. Goyret, M. von Arx, C. T. Pierce, J. L. Bronstein *et al.*, 2013 The effect of ambient
842 humidity on the foraging behavior of the hawkmoth Manduca sexta. Journal of Comparative
843 Physiology A 199: 1053–1063.
844 Danecek, P., A. Auton, G. Abecasis, C. A. Albers, E. Banks *et al.*, 2011 The variant call format and
845 VCFtools. Bioinformatics 27: 2156–2158.
846 Dobzhansky, T., and A. H. Sturtevant, 1938 Inversions in the chromosomes of Drosophila pseudoobscura.
847 Genetics 23: 28.
848 Evanno, G., S. Regnaut, and J. Goudet, 2005 Detecting the number of clusters of individuals using the
849 software STRUCTURE: a simulation study. Molecular ecology 14: 2611–2620.
850 Ferguson, D., 1991 An essay on the long-range dispersal and biogeography of Lepidoptera, with special
851 reference to the Lepidoptera of Bermuda. Memoirs of the Entomological Society of Canada 158:
852 67–79.
853 Fuller, Z. L., S. A. Koury, N. Phadnis, and S. W. Schaeffer, 2019 How chromosomal rearrangements shape
854 adaptation and speciation: Case studies in Drosophila pseudoobscura and its sibling species
855 Drosophila persimilis. Molecular ecology 28: 1283–1301.
856 Gershman, A., T. G. Romer, Y. Fan, R. Razaghi, W. A. Smith *et al.*, 2021 De novo genome assembly of the
857 tobacco hornworm moth (Manduca sexta). G3 11: jkaa047.
858 Grabherr, M. G., P. Russell, M. Meyer, E. Mauceli, J. Alföldi *et al.*, 2010 Genome-wide synteny through
859 highly sensitive sequence alignment: Satsuma. Bioinformatics 26: 1145–1151.

Haber, W. A., and G. W. Frankie, 1989 A tropical hawkmoth community: Costa Rican dry forest Sphingidae. Biotropica 155–172.

Höglund, G., and G. Struwe, 1970 Pigment migration and spectral sensitivity in the compound eye of moths. Zeitschrift für vergleichende Physiologie 67: 229–237.

Janzen, D. H., 1984 Two ways to be a tropical big moth: Santa Rosa saturniids and sphingids.

Kanost, M. R., E. L. Arrese, X. Cao, Y.-R. Chen, S. Chellapilla *et al.*, 2016 Multifaceted biological insights from a draft genome sequence of the tobacco hornworm moth, *Manduca sexta*. Insect Biochemistry and Molecular Biology 76: 118–147.

Kanost, M. R., H. Jiang, and X. Q. Yu, 2004 Innate immune responses of a lepidopteran insect, *Manduca sexta*. Immunological Reviews 198: 97–105.

Kapun, M., D. K. Fabian, J. Goudet, and T. Flatt, 2016 Genomic evidence for adaptive inversion clines in Drosophila melanogaster. Molecular biology and evolution 33: 1317–1336.

Kawahara, A. Y., J. W. Breinholt, F. V. Ponce, J. Haxaire, L. Xiao *et al.*, 2013 Evolution of Manduca sexta hornworms and relatives: Biogeographical analysis reveals an ancestral diversification in Central America. Molecular Phylogenetics and Evolution 68: 381–386.

Kirkpatrick, M., and N. Barton, 2006 Chromosome inversions, local adaptation and speciation. Genetics 173: 419–434.

Knief, U., G. Hemmrich-Stanisak, M. Wittig, A. Franke, S. C. Griffith *et al.*, 2016 Fitness consequences of polymorphic inversions in the zebra finch genome. Genome biology 17: 199.

Kopelman, N. M., J. Mayzel, M. Jakobsson, N. A. Rosenberg, and I. Mayrose, 2015 Clumpak: a program for identifying clustering modes and packaging population structure inferences across K. Molecular ecology resources 15: 1179–1191.

Korneliussen, T. S., A. Albrechtsen, and R. Nielsen, 2014 ANGSD: Analysis of Next Generation Sequencing Data. BMC Bioinformatics 15:.

Kryuchkova-Mostacci, N., and M. Robinson-Rechavi, 2017 A benchmark of gene expression tissue-specificity metrics. Briefings in Bioinformatics 18: 205–214.

Lande, R., 1984 The expected fixation rate of chromosomal inversions. Evolution 743–752.

Langmead, B., and S. L. Salzberg, 2012 Fast gapped-read alignment with Bowtie 2. Nat Methods 9: 357–359.

Lasne, C., C. M. Sgrò, and T. Connallon, 2017 The Relative Contributions of the X Chromosome and Autosomes to Local Adaptation. Genetics 205: 1285–1304.

Lee, Y. W., L. Fishman, J. K. Kelly, and J. H. Willis, 2016 A segregating inversion generates fitness variation in yellow monkeyflower (Mimulus guttatus). Genetics 202: 1473–1484.

Lou, R. N., A. Jacobs, A. Wilder, and N. O. Therkildsen, 2020 A beginner's guide to low-coverage whole genome sequencing for population genomics.

Lunter, G., and M. Goodson, 2011 Stampy: A statistical algorithm for sensitive and fast mapping of Illumina sequence reads. Genome Research 21: 936–939.

Lyons, J. I., A. A. Pierce, S. M. Barribeau, E. D. Sternberg, A. J. Mongue *et al.*, 2012 Lack of genetic differentiation between monarch butterflies with divergent migration destinations. Molecular Ecology 21: 3433–3444.

McKenna, A. H., M. Hanna, E. Banks, A. Sivachenko, K. Cibulskis *et al.*, 2010 The Genome Analysis Toolkit: A MapReduce framework for analyzing next-generation DNA sequencing data. Genome Research 20: 1297–1303.

McNeil, J., 1995 Physiological integration of migration in Lepidoptera. Insect migration: tracking resources through space and time.

Mechaber, W. L., and J. G. Hildebrand, 2000 Novel, non-solanaceous hostplant record for Manduca sexta (Lepidoptera: Sphingidae) in the Southwestern United States. Annals of the Entomological Society of America 93: 447–451.

908 Meisner, J., and A. Albrechtsen, 2018 Inferring population structure and admixture proportions in low-
909 depth NGS data. Genetics 210: 719–731.
910 Mérot, C., E. Berdan, H. Cayuela, H. Djambazian, A.-L. Ferchaud *et al.*, 2021 Locally adaptive inversions
911 modulate genetic variation at different geographic scales in a seaweed fly. bioRxiv 2020–12.
912 Mongue, A. J., M. E. Hansen, L. Gu, C. E. Sorenson, and J. R. Walters, 2019 Nonfertilizing sperm in
913 Lepidoptera show little evidence for recurrent positive selection. Molecular Ecology 28: 2517–
914 2530.
915 Mongue, A. J., M. E. Hansen, and J. R. Walters, 2021 Support for faster and more adaptive Z
916 chromosome evolution in two divergent lepidopteran lineages. Evolution n/a:
917 Mongue, A. J., M. E. Hansen, and J. R. Walters, 2020 ZZ Top: faster and more adaptive Z chromosome
918 evolution in two Lepidoptera. bioRxiv.
919 Mongue, A. J., and J. Walters, 2017 The Z chromosome is enriched for sperm proteins in two divergent
920 species of Lepidoptera. Genome 61: 248–253.
921 Nardi, J. B., 1993 Modulated expression of a surface epitope on migrating germ cells of Manduca sexta
922 embryos. Development 118: 967–975.
923 Nei, M., 1987 *Molecular evolutionary genetics*. Columbia university press.
924 Nei, M., Y. Niimura, and M. Nozawa, 2008 The evolution of animal chemosensory receptor gene
925 repertoires: roles of chance and necessity. Nature Reviews Genetics 9: 951–963.
926 Prieto-Godino, L. L., R. Rytz, B. Bargeton, L. Abuin, J. R. Arguello *et al.*, 2016 Olfactory receptor pseudo-
927 pseudogenes. Nature 539: 93–97.
928 R Core Team, 2017 R Core Team (2017). R: A language and environment for statistical computing. R
929 Foundation for Statistical Computing, Vienna, Austria. URL http://www.R-project.org/. R
930 Foundation for Statistical Computing.
931 Rausch, T., T. Zichner, A. Schlattl, A. M. Stütz, V. Benes *et al.*, 2012 DELLY: structural variant discovery by
932 integrated paired-end and split-read analysis. Bioinformatics 28: i333–i339.
933 Rice, W. R., 1984 Sex chromosomes and the evolution of sexual dimorphism. Evolution 38: 735–742.
934 Shapiro, A. M., 2006 Survival of freezing and subsequent summer eclosion by three migratory moths:
935 Manduca sexta and Hyles Lineata (Sphingidae), and Helicoverpa zea (Noctuidae). Journal of the
936 Lepidopterists' Society 60: 101–103.
937 Skotte, L., T. S. Korneliussen, and A. Albrechtsen, 2013 Estimating individual admixture proportions from
938 next generation sequencing data. Genetics 195: 693–702.
939 Stevenson, R., K. Corbo, L. Baca, and Q. Le, 1995 Cage size and flight speed of the tobacco hawkmoth
940 Manduca sexta. Journal of Experimental Biology 198: 1665–1672.
941 Sturtevant, A. H., 1917 Genetic factors affecting the strength of linkage in Drosophila. Proceedings of the
942 National Academy of Sciences of the United States of America 3: 555.
943 The International Silkworm Genome Consortium, 2008 The genome of a lepidopteran model insect, the
944 silkworm *Bombyx mori*. Insect Biochemistry and Molecular Biology 38: 1036–1045.
945 Todesco, M., G. L. Owens, N. Bercovich, J.-S. Légaré, S. Soudi *et al.*, 2020 Massive haplotypes underlie
946 ecotypic differentiation in sunflowers. Nature 584: 602–607.
947 Wagner, D. L., 2005 *Caterpillars of eastern North America: a guide to identification and natural history*.
948 Princeton University Press.
949 Wellenreuther, M., H. Rosenquist, P. Jaksons, and K. W. Larson, 2017 Local adaptation along an
950 environmental cline in a species with an inversion polymorphism. Journal of Evolutionary
951 Biology 30: 1068–1077.
952 Whittington, E., Q. Zhao, K. Borziak, J. R. Walters, and S. Dorus, 2015 Characterisation of the *Manduca*
953 *sexta* sperm proteome: Genetic novelty underlying sperm composition in Lepidoptera. Insect
954 Biochemistry and Molecular Biology 62: 183–193.

955 Wysoker, A., K. Tibbetts, and T. Fennell, 2013 Picard tools version 1.90. http://picard. sourceforge. net
956 (Accessed 14 December 2016) 107: 308.
957 Yasukochi, Y., M. Tanaka-Okuyama, F. Shibata, A. Yoshido, F. Marec *et al.*, 2009 Extensive conserved
958 synteny of genes between the karyotypes of *Manduca sexta* and *Bombyx mori* revealed by BAC-
959 FISH mapping. PLoS ONE 4: e7465:
960 Zhan, S., W. Zhang, K. Niitepõld, J. Hsu, J. F. Haeger *et al.*, 2014 The genetics of monarch butterfly
961 migration and warning colouration. Nature 514: 317–321.
962 Zhang, Z.-J., S.-S. Zhang, B.-L. Niu, D.-F. Ji, X.-J. Liu *et al.*, 2019 A determining factor for insect feeding
963 preference in the silkworm, Bombyx mori. PLOS Biology 17: e3000162.
964
965
966
967
968
969
970
971
972
973
974
975
976
977
978
979
980
981
982
983
984
985
986

987 Supplementary tables and figures
988

Putative chromosome	Kanost *et al.* Scaffold	Gershman et al. Scaffold	Type
Z	scaffold00022	HiC_scaffold_19	Inversion
12	scaffold00042	HiC_scaffold_12	Inversion
12	scaffold00095	HiC_scaffold_12	Inversion
12	scaffold00119	HiC_scaffold_12	Inversion
12	scaffold00158	HiC_scaffold_12	Inversion
12	scaffold00203	HiC_scaffold_12	Inversion
12	scaffold00240	HiC_scaffold_12	Inversion
12	scaffold00264	HiC_scaffold_12	Inversion
12	scaffold00300	HiC_scaffold_12	Inversion
12	scaffold00335	HiC_scaffold_12	Inversion
12	scaffold00460	HiC_scaffold_12	Inversion
12	scaffold00466	HiC_scaffold_12	Inversion
12	scaffold00571	HiC_scaffold_12	Inversion
12	scaffold00616	HiC_scaffold_12	Inversion
12	scaffold00633	HiC_scaffold_12	Inversion
12	scaffold00790	HiC_scaffold_12	Inversion
12	scaffold00888	HiC_scaffold_12	Inversion
12	scaffold00921	HiC_scaffold_12	Inversion
12	scaffold00966	HiC_scaffold_12	Inversion
12	scaffold01138	HiC_scaffold_12	Inversion
12	scaffold01198	HiC_scaffold_12	Inversion
12	scaffold01282	HiC_scaffold_12	Inversion
12	scaffold01317	HiC_scaffold_12	Inversion
12	scaffold01366	HiC_scaffold_12	Inversion
12	scaffold01482	HiC_scaffold_12	Inversion
12	scaffold01552	HiC_scaffold_12	Inversion
12	scaffold00381	HiC_scaffold_12	Inversion, potential pseudogene
19	scaffold00118	HiC_scaffold_21	Localized peak
19	Scaffold00419	HiC_scaffold_21	Localized peak

989

990 **Table S1.** Scaffold information for genomic regions of interest. To be included in this table, a scaffold
991 had to show at least one 10 kilobase window in which F_{ST} was greater than 0.5 between any two of the 3
992 populations. The **Type** of differentiation (e.g. localize peak vs. inversion) was determined through
993 subsequent analyses. For convenience, genomic locations are provided for both assemblies of *M. sexta*.

994

995

Genotype	Chr12_inversion	Stop-loss variant	Z inversion	Chr19_oddities
+/+	A36, A70, A78, A82	A36, A70, A78, A82	A36, A70, A71*, A78, A82, A84, A85	A70, A71, A76, A78, A84
+/-	A71, A76, A84	A71, A76, A84		A85
-/-	A85	A85	A76*	A36, A82

Table S2. Genotypes of Arizona individuals for each of the key variants discussed in this manuscript. + denotes presence, - absence. The stop-loss variant and chromosome 12 inversion co-segregate in perfect linkage, further proof that the former resides within the latter. The Z inversion is not structured in the same way, however. Individuals marked with an * are female and hemizygous. Thus A71's single Z carries the inversion while A76's lacks it.

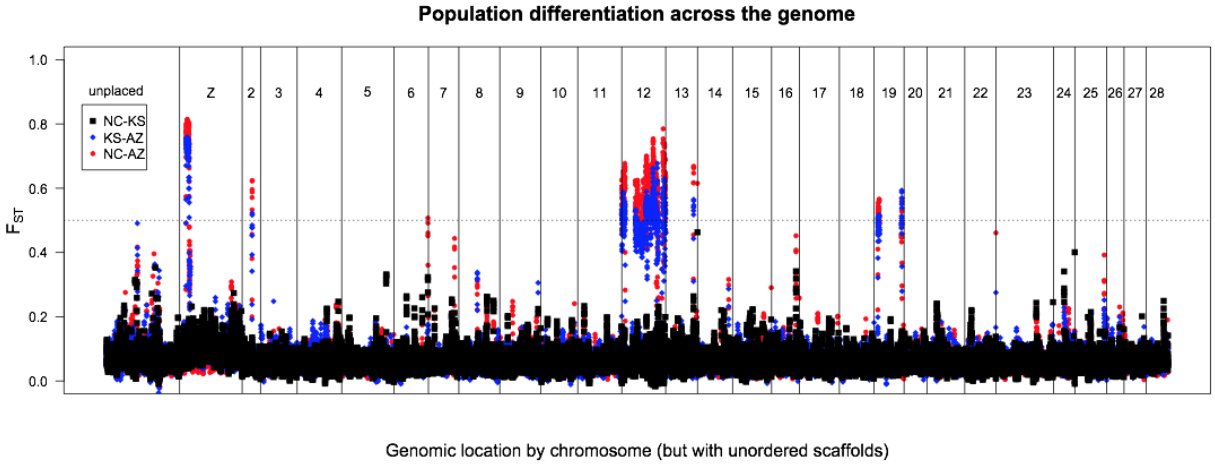

Figure S1. Pairwise differentiation (F_{ST}) across the *M. sexta* genome using the Kanost *et al.* reference: North Carolina (NC) vs. Kansas (KS; black squares), Kansas vs. Arizona (AZ; blue diamonds), and North Carolina vs. Arizona (red points). Plotting is ordered by chromosomal linkage, but not ordered within a chromosome. We examined regions of differentiation greater than 0.5 (dashed line). By this metric, one peak on the Z, and one peak each on chromosomes 2, 13, and two on 19. Additionally, note the massive spike on chromosome 12, made up of numerous highly differentiated scaffolds. Some assignments, especially the peak on chromosome 13, were updated in the new assembly.

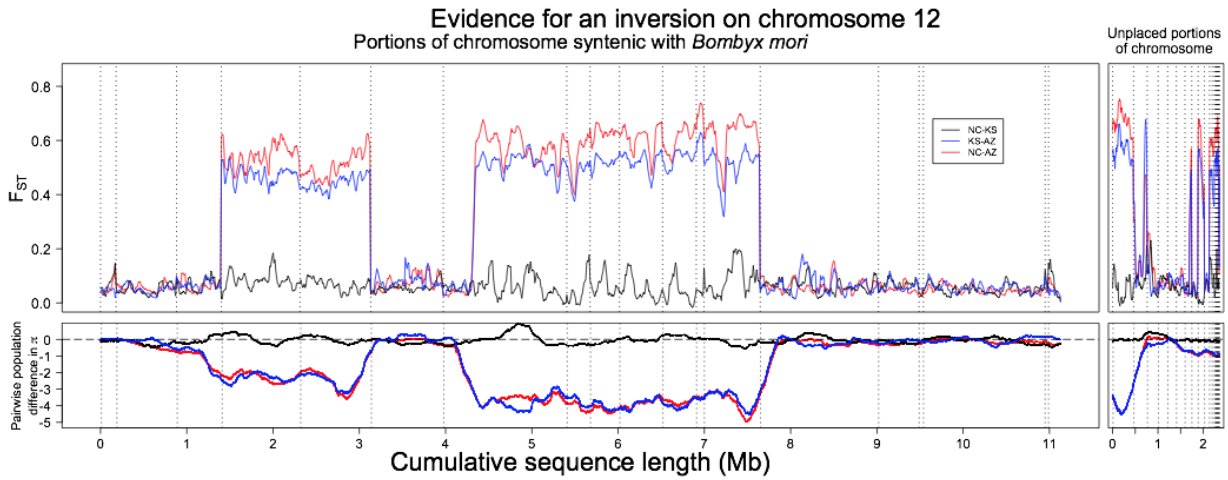

Figure S2. Investigation of differentiation across chromosome 12. **Top:** Ordering scaffolds from **Figure S1** via synteny with *Bombyx mori* suggests two regions > 1.5 Mb of elevated differentiation (F_{ST}) between *M. sexta* populations. Given the wholly contiguous nature of the signal in the Gershman et al. assembly, this arrangement is best understood as an intra-chromosomal rearrangement between *Manduca* and *Bombyx* leading to an incorrect synteny ordering. **Bottom:** Examining deviations from background levels of variation with pairwise difference in genetic diversity (π) between populations. Diversity is roughly equal between populations (near 0 difference) except within putatively inverted regions, in which both NC and KS have fewer pairwise differences than AZ. In both the top and bottom, scaffold limits are denoted by dashed vertical lines. **Left:** The majority of assembled scaffolds could be placed in an order with synteny. **Right:** Some scaffolds could not be placed by this method and appear here, unordered. Note that some among these scaffolds also show scaffold-wide differentiation and differences in diversity. Compare to Figure 4 of the main text, in which the full length of the putative inversion appears to have been contiguously assembled.

1040

1041

1042

1043

1044

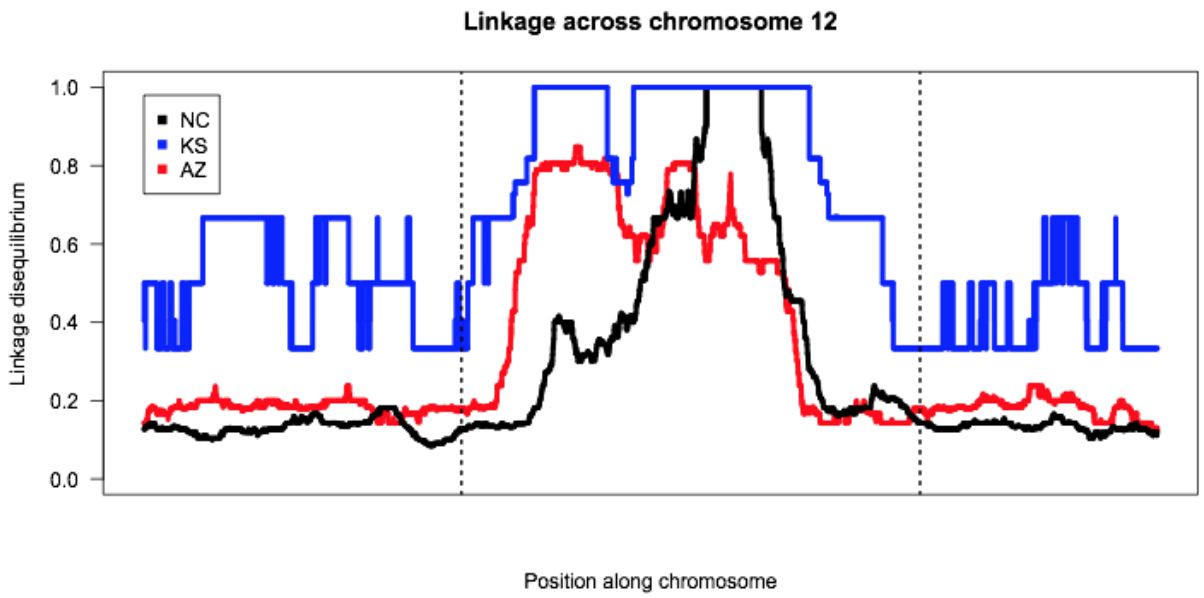

1045

1046 **Figure S3.** Linkage disequilibrium across chromosome 12. A rolling median of windows of 10Kb for the
1047 genotype ρ^2 as calculated with vcftools in each population. Dashed lines indicate approximate location
1048 of the inferred inversion breakpoints. Note as well with the fewest sampled chromosomes in the Kansas
1049 population, apparent linkage is overall higher across the chromosome.

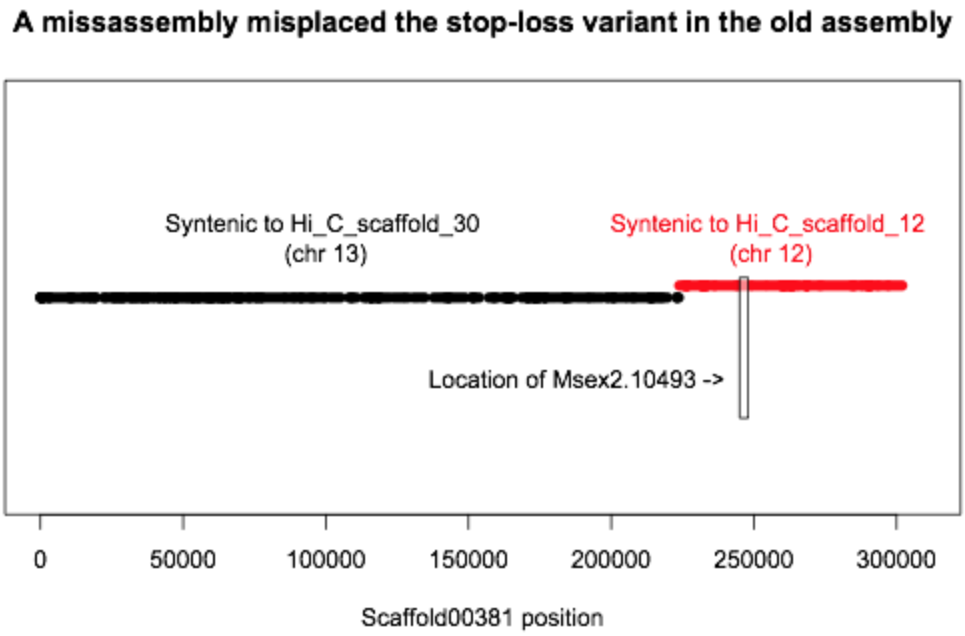

1050

1051 **Figure S4.** Syntenic alignment of scaffold00381 compared to the chromosome-level assembly. The
1052 majority of the scaffold (in black) is syntenic to chromosome 13, explaining its previous assignment to
1053 that chromosome. However, a significant portion of the sequence (red), including Msex2.10493, the
1054 putative segregating pseudogene, is syntenic to chromosome 12.

1055

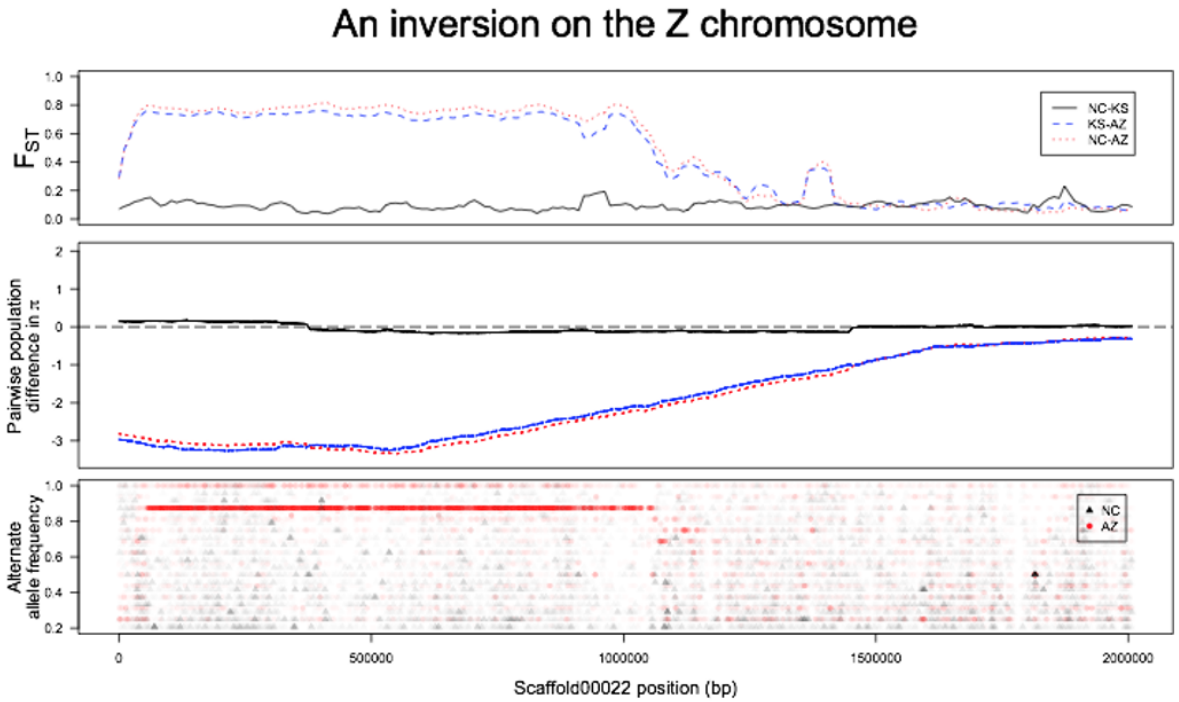

Figure S5. Evidence for an inversion on the Z chromosome using the Kanost et al. assembly. **Top.** A roughly 1 Mb portion of scaffold0002 (from 58 Kb to 1.03 Mb) shows elevated differentiation in North Carolina – Arizona and Kansas – Arizona comparisons. **Middle.** As with the chromosome 12 inversion, this region shows differences in π between the inverted and non-inverted region. **Bottom.** Like the chromosome 12 inversion, Arizona shows a long tract of shared allele frequencies in the region while North Carolina does not (note that Kansas allele frequencies are omitted due to lower sampling effort artificially stratifying frequencies).

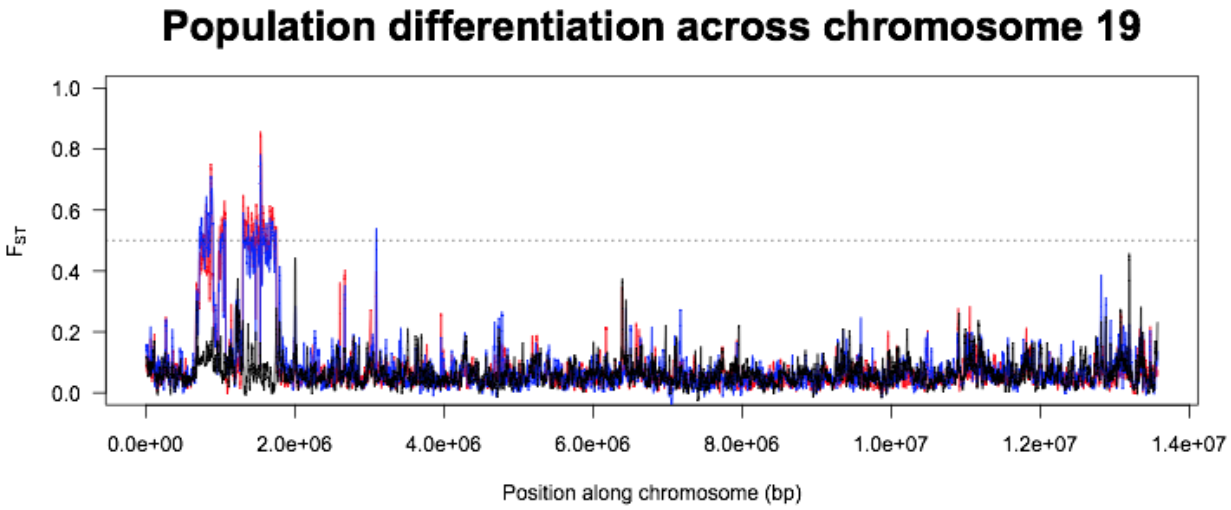

1075

1076 **Figure S6.** Population differentiation on chromosome 19. Two separate regions of elevated F_{ST} occur in
1077 the first two megabases of the chromosome, corresponding to the two different outlier scaffolds in the
1078 Kanost et al. assembly.